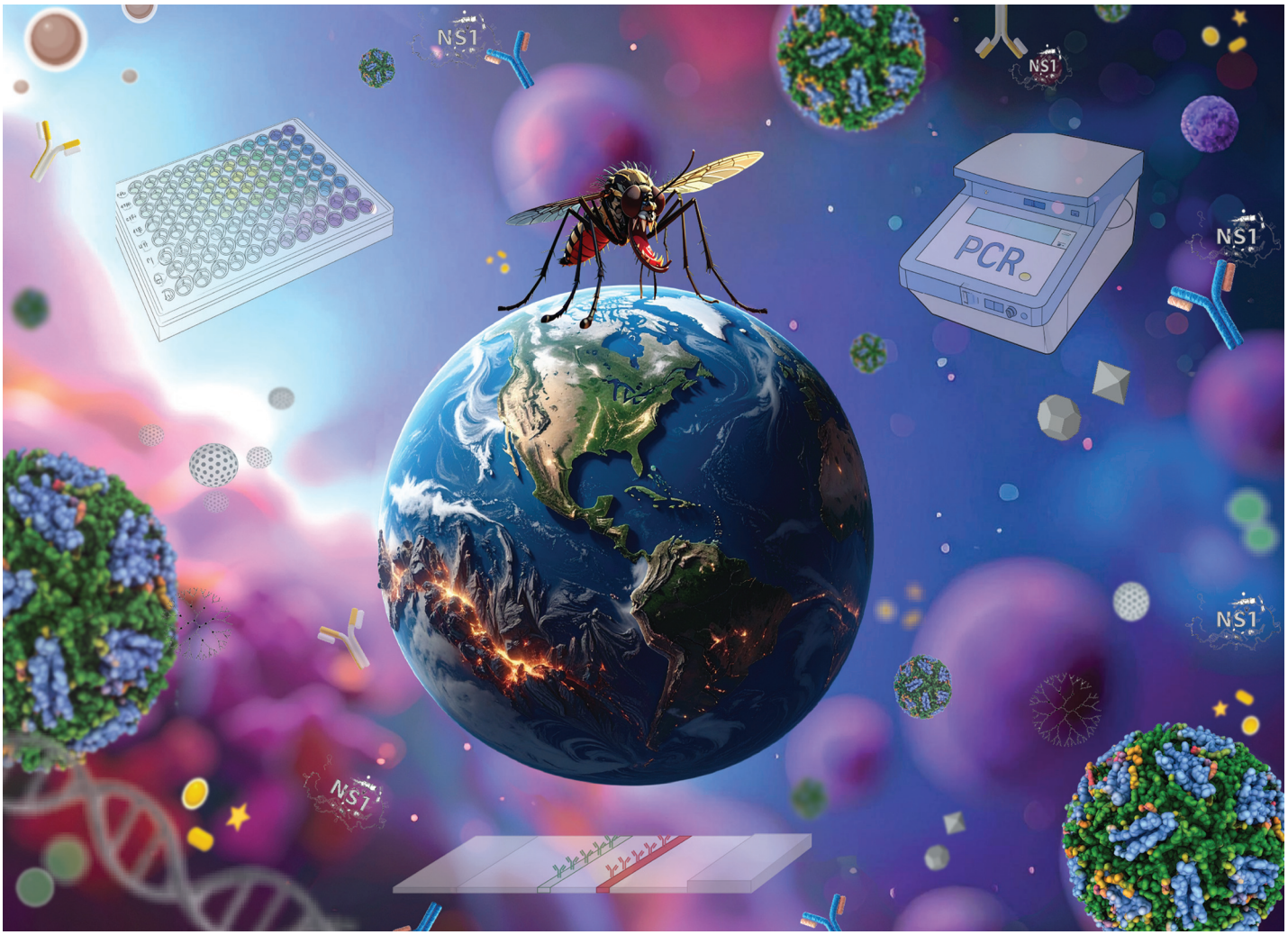

Showcasing research from Professor Nguyen Thi Kim Thanh's laboratory, UCL Healthcare Biomagnetics and Nanomaterials Laboratories, Biophysics Group, University College London, United Kingdom, and Dr Xiaodi Su's laboratory, Institute of Material Research and Engineering, A*STAR, Singapore.

Dengue diagnostics: from commercial tests to optical nanosensors

This work reviews optical nanosensor-based Dengue virus detection, whilst also summarising current diagnostic methods. The nanosensors are classified by the nanoparticles' colourimetric, surface plasmon resonance (SPR)/localised SPR, fluorescence, evanescent wave transmission and surface-enhanced Raman spectroscopy characteristics. The optical principles of the sensors and the sensor performance for various dengue infection analytes are critically reviewed. Finally, the key gaps in Dengue virus detection are highlighted and future directions for enhanced performance nanoparticle-based optical testing are proposed.

Image reproduced by permission of Rhai-Anne A. C. Etienne and Nguyen Thi Kim Thanh

As featured in:

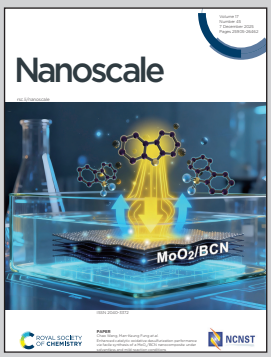

See Xiaodi Su, Nguyen Thi Kim Thanh *et al.*, *Nanoscale*, 2025, **17**, 25920.

ROYAL SOCIETY OF CHEMISTRY

rsc.li/nanoscale

Registered charity number: 207890

Nanoscale

REVIEW

View Article Online
View Journal | View Issue

Cite this: *Nanoscale*, 2025, **17**, 25920

Dengue diagnostics: from commercial tests to optical nanosensors

Rhai-Anne A. C. Etienne, [a,b,c] Yasuhiro Takeuchi, [d,e] Xiaodi Su *[c,f] and Nguyen Thi Kim Thanh *[a,b]

Dengue virus (DENV) infections are a globally recognised problem, and the development of sensitive, accurate and affordable diagnostic tests is required for better epidemic control and mitigation of mortality and morbidity. With the increasing use of nanoparticles (NPs) in diagnostics, nanoparticle-based optical biosensors emerged as a convenient choice due to their simplicity and potential to satisfy the criteria for an ideal diagnostic test. The optical nanosensors are classified by the colourimetric, surface plasmon resonance (SPR)/localised SPR (LSPR), fluorescence, evanescent wave transmission and surface-enhanced Raman spectroscopy (SERS) characteristics of the NPs. Various NPs, including gold, silver, carbon, iron oxide, and poly(amidoamine) (PAMAM), can be used as signalling materials to enhance test performances. For a critical comparison, target analytes, the basis of the sensor and the performance (limit of detection (LOD), sensitivity, specificity, cross-reactivities) are reviewed. The background information regarding DENV infection progression and the demand for diagnostics at different infection stages allows for a comprehensive understanding of the requirements for useful dengue diagnostic tests. Highlighting the performance strengths and limitations of laboratory-based molecular tests, immunoassays, and rapid diagnostic tests (RDTs) would permit the development of a future strategy in designing a better home-based DENV test.

Received 5th May 2025,
Accepted 4th September 2025

DOI: 10.1039/d5nr01842k

rsc.li/nanoscale

1. Introduction

Dengue is an endemic disease responsible for causing dengue fever.[1] The etiological agent dengue virus (DENV) is an arthropod-borne member of the family Flaviviridae, genus Flavivirus. There are four serotypes, DENV-1, DENV-2, DENV-3, and DENV-4. The prevalence of each serotype varies depending on the region.[2] DENV is spread by receiving a bite from an infected *Aedes* mosquito, the prevalence and persistence of these mosquitoes is responsible for the expansion of infections.[3] A multitude of other contributing factors drive up the viral contraction rate *i.e.* global warming, poor global health standards, insufficient mosquito control, and frequent worldwide travel all play a role.[2] Approximately 60% of the global population is at risk of developing dengue fever. From the beginning of 2025, there have been over 1.4 million confirmed DENV cases and more than 400 deaths globally.[4] It is predicted that an additional ~2.25 billion people will incur the risk of developing the disease in 2080 compared to 2015.[5] The recent distribution of DENV infections is indicated in Fig. 1.[6] This arbovirus is prevalent in sub-tropical and tropical regions, areas known to have limited access to gold-standard healthcare. Thus indicating the importance of an affordable and quick dengue diagnostic test.[1,7]

DENV infections are not only systemic but also dynamic due to the fluctuations in clinical manifestations. Infections are either asymptomatic or symptomatic, with symptom complexity varying vastly from minor to severe. Treatment is cheap, effective and straightforward,[8,9] but is heavily reliant on intervening at the right time during DENV infection progression. A good clinical frontline response would help lower non-essential hospital admissions, in addition to providing early detection.[9] Therefore, the efficiency and accuracy of dengue diagnostics are of utmost importance, especially in the early stages of the infection.[1]

[a]*Biophysics Group, Department of Physics and Astronomy, University College London, UK*
[b]*UCL Healthcare Biomagnetics and Nanomaterials Laboratories, The Royal Institution, 21 Albemarle Street, London, W1S 4BS, UK. E-mail: ntk.thanh@ucl.ac.uk; https://www.ntk-thanh.co.uk*
[c]*Institute of Materials Research and Engineering, A*STAR (Agency for Science, Technology and Research), 2 Fusionopolis Way, Innovis, #8-03, Singapore 138634, Singapore*
[d]*Division of Infection and Immunity, University College London, Cruciform Building, Gower Street, London WC1E 6BT, UK*
[e]*Biotherapeutics and Advanced Therapies, Scientific Research and Innovation, Medicines and Healthcare products Regulatory Agency, South Mimms EN6 3QC, Potters Bar, UK*
[f]*Department of Chemistry, National University of Singapore, Singapore 117543, Singapore. E-mail: xd-su@imre.a-star.edu.sg*

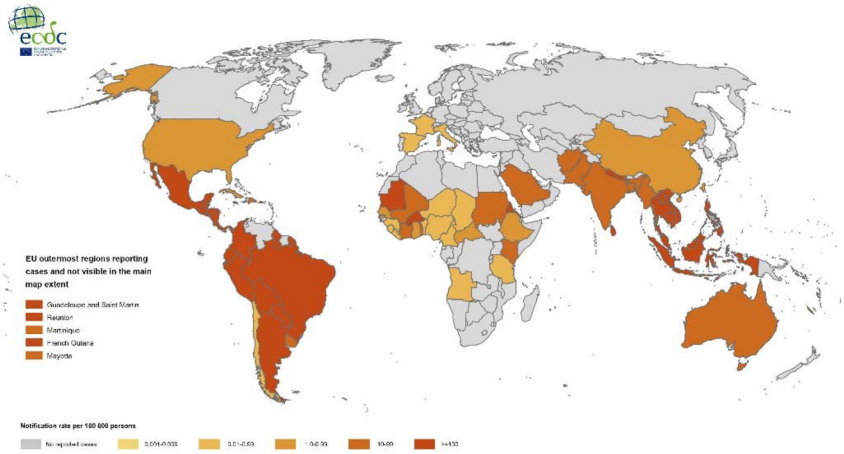

Fig. 1 Global distribution of dengue virus infections from August 2024–July 2025, using the DENV case notification rate per 100 000 population. Sourced from European Centre for Disease Prevention and Control. The map was produced on the 17th July 2025.[6] © ECDC [2025], CC BY 4.0.

Many questions still surround diagnostic improvements. Our review highlights key aspects, including current efforts for diagnosing DENV infections and recent developments in the field. Reviews published between 2019 and 2024 only focus on general electrical and optical-based bench diagnostics, but do not cover NP-based sensing.[10–12] Therefore, the main objective of this review is to evaluate the commercially available tests and compare examples of DENV optical biosensors where NPs form the basis for signal transduction. By highlighting the sensitivities and specificities of the most popular RDTs,[13] and investigating the circulating antigenemia of non-structural protein 1 (NS1), we provide a more in-depth view of the current diagnostic detection limits, which may aid in identifying appropriate pathways for developing an ideal DENV test.

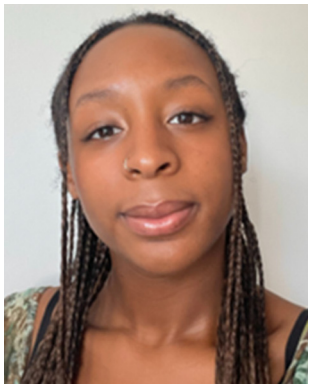

Rhai-Anne A. C. Etienne

*Rhai-Anne received a first class honours MChem in Medicinal Chemistry with Pharmacology from the University of Liverpool (2023). During her integrated master's, she explored the synthesis of Anti-Cryptococcal agents, predominantly working with imines and quinolines, under the supervision of Dr Gemma Nixon at the University of Liverpool. She also explored antibiotic enhancement using peptide chains under the supervision of Dr Ishwar Singh at the University of Liverpool. Rhai-Anne's research interests lie in medicinal chemistry and nanomaterials for infectious disease diagnosis. She is an A*STAR ARAP PhD student studying at University College London and the A*STAR Institute of Materials Research and Engineering in Singapore (IMRE). Her doctoral research focuses on the development of a rapid diagnostic test using nanoparticles, under the supervision of Prof. Nguyen Thi Kim Thanh at UCL and Xiaodi Su at A*STAR IMRE.*

Yasuhiro Takeuchi

Yasuhiro is an Associate Professor of Molecular Virology at the Division of Infection and Immunity, UCL. He's been based in London for 33 years, initially at the Institute of Cancer Research and then UCL. He studied Biochemistry at the University of Tokyo and obtained an MSc on the physicochemical study of nucleic acids, and then a PhD on molecular biology of small nuclear RNA. He started his research on retroviruses on being appointed as a junior lecturer at Gunma University, Japan in 1986. Since then he's been working on human viruses, HIV and HTLV and mammalian gammaretroviruses, including porcine endogenous retroviruses. His research on retrovirus biology has involved several aspects of infection and evolution with an emphasis on envelope-receptor interaction. The applied side of his research has focused on the use of retroviruses as vectors for gene therapy, pandemic preparedness against emerging viruses and zoonotic infection in xenotransplantation. In September 2016 he started a secondment for 30% of the time in the Advanced Therapy Division in NIBSC (presently, Biotherapeutics and Advanced Therapies, Scientific Research and Innovation, Medicines and Healthcare products regulatory agency).

2. Disease progression and biomarkers

DENV infections result in a wide range of disease outcomes, from asymptomatic, mild febrile illness, and severe dengue fever to death. As a somewhat DENV-specific phenomenon, the disease course can depend on previous infections.[14]

Disease dynamics of mild, self-resolving cases provide some knowledge of the disease progression and biomarker development. After being bitten, an incubation period averaged at 6 d occurs,[15] after which, symptoms may present themselves. The dengue life cycle, shown in Fig. 2, details the viral genome translation that occurs following the viral particles' entry into the host cells. Both viral structural and non-structural proteins are produced; the three structural proteins (Capsid, Membrane, Envelope) are included in the mature virion particles, and the seven non-structural proteins (NS1, NS2A, NS2B, NS3, NS4A, NS4B, and NS5) aid in viral particle replication.[16,17] The pathogenesis of DENV infections is influenced by multiple mechanisms, see Fig. 2.[16,18] The host responses to virus replication and viral antigen production affect pathogenesis and encompass antibody-dependent enhancement (ADE), anti-NS1 antibodies, autoimmunity and memory cross-reactive T-cells, whereas viral factors are linked to the DENV NS1 and genome variations.[16,18,19] The pathogenesis of severe dengue has been heavily associated with detrimental host responses in addition to viral virulence factors,

Xiaodi Su

*Xiaodi Su obtained her PhD degree (Analytical Chemistry) from Nankai University, China (1995). Currently, she is a Senior Principal Scientist and a group leader (BioNanoSensors) at the Institute of Materials Research and Engineering (IMRE), Agency for Science, Technology and Research (A*STAR), Singapore. She is also an Adjunct Professor in the Chemistry Department of the National University of Singapore (NUS). Her research interests include nanobiotechnology, nanomaterials for biomedical applications, infectious disease diagnosis, environmental biosurveillance, and food security. Her research expertise includes biophysical characterisation of biomolecular interactions, nanomaterials synthesis and biofunctionalisation, bioassay designs, optical biosensors, and Lateral Flow Assay development etc. She has authored/co-authored 150 publications in international peer-reviewed journals. She serves on the Editorial Advisory Board of ACS Applied Nanomaterials.*

Nguyen Thi Kim Thanh

Professor Nguyen Thi Kim Thanh, MAE, FRSC, FInstP, FAPS, FIMMM FRSB (https://www.ntk-thanh.co.uk) held a prestigious Royal Society University Research Fellowship (2005–2014). She was appointed a Full Professor in Nanomaterials in 2013 at University College London. She leads a very dynamic group conducting cutting-edge interdisciplinary and innovative research on the design and synthesis of magnetic and plasmonic nanomaterials, mainly for biomedical applications. In 2019, she was honoured for her achievements in the field of nanomaterials and was awarded the highly prestigious Royal Society Rosalind Franklin Medal. She was RSC Interdisciplinary Prize winner in 2022. She was awarded SCI/RSC Colloids Groups 2023 Graham Prize Lectureship to recognise an outstanding mid-career researcher in colloid and interface science. She is one of 12 recipients globally of 2023 Distinguished Women in Chemistry/Chemical Engineering Awards, bestowed by the International Union of Pure and Applied Chemistry (IUPAC). Currently, she is Vice Dean for Innovation and Enterprise at the Faculty of Maths and Physical Sciences. She was elected as a member of Academia Europaea in April 2024. She is Editor-in chief of the Royal Society of Chemistry book Series, Nanoscience and Nanotechnology and an Associate Editor for Nanoscale and Nanoscale Advances Journals. She edited 8 theme issues including: Design and scaling up of theragnostic nanoplatforms for health: towards translational studies. Nanoscale, RSC (2023); Theragnostic nanoplatforms for biomedicine Nanoscale, RSC (2021); Multifunctional nanostructures for diagnosis and therapy of diseases. Interface Focus, The Royal Society (2016). She is the sole editor of two seminal books on Magnetic Nanoparticles from Fabrication to Clinical Applications (https://tinyurl.com/y5bgxb3r) and Clinical Applications of Magnetic nanoparticles (https://tinyurl.com/yyjawnz2).

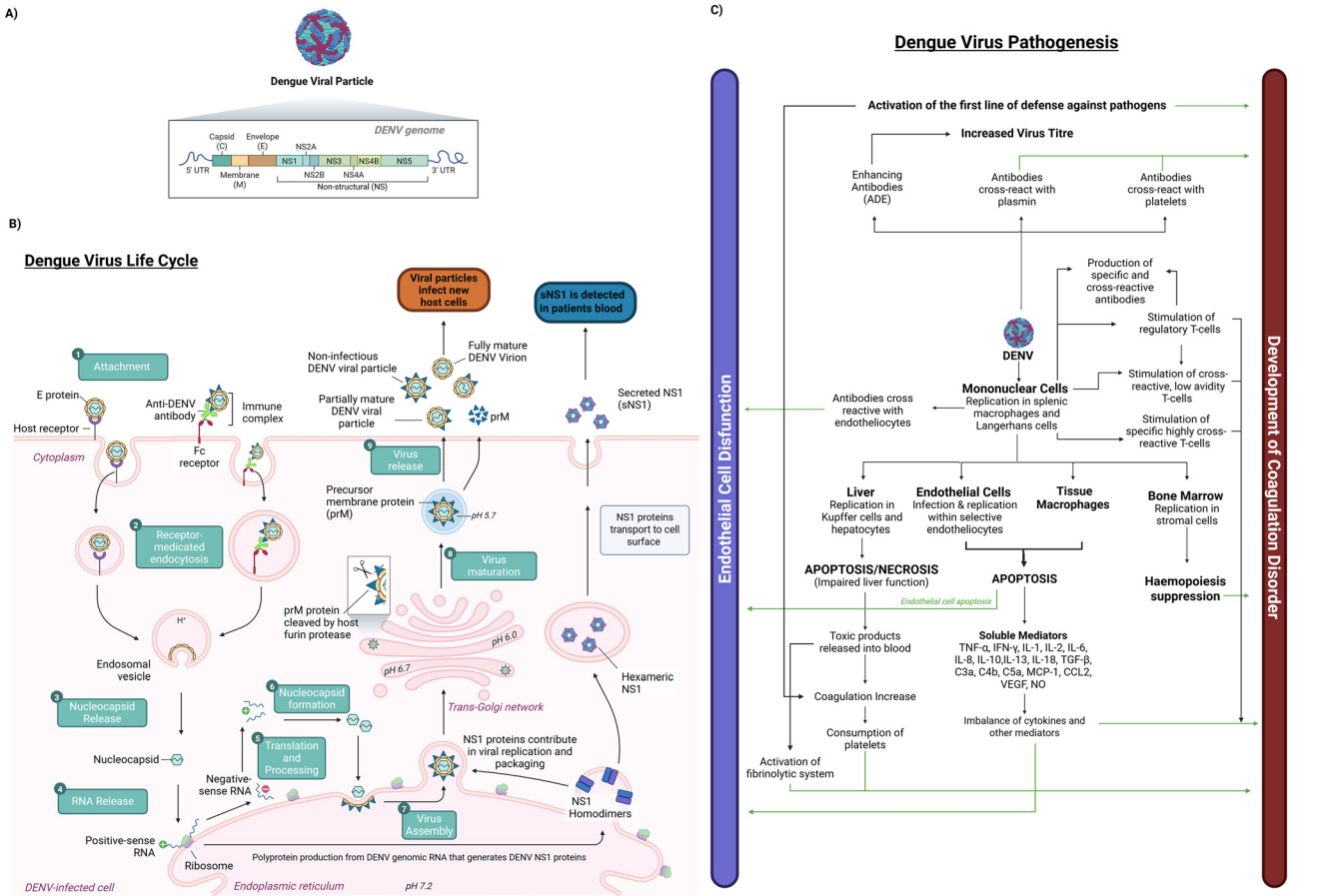

Fig. 2 Schematic diagram of the structural organisation of the DENV genome, the DENV viral life cycle and the pathogenesis of DENV infections, created in BioRender. Etienne, R. (2025) https://BioRender.com/ndsc5ym. (A) DENV genome is comprised of the 5′UTR, ORF, and 3′UTR. The three structural proteins: C (Capsid), M (Membrane) and E (Envelope), alongside the seven non-structural proteins (NS1, NS2A, NS2B, NS3, NS4A, NS4B, NS5) are processed from the polyprotein translated from the ORF.[16] (B) DENV replication starts with viral particle entry into the host cell, either through the Fc receptors that attach to the Fc region of the DENV particle-antibody immunocomplex or by a range of host cell receptors. (1) DENV particle attaches to receptors. (2) Receptor-mediated endocytosis occurs, *via* endosomes and following a pH decrease, genome uncoating occurs. (3) Endosomes undergo a conformational change to release the nucleocapsid into the cytoplasm. (4) Viral RNA is released into cytoplasm following nucleocapsid disassembly. (5) Viral RNA translocates into the Endoplasmic Reticulum (ER) and is translated into a polyprotein, where the host proteases and non-structural 2B (NS2B) or NS3 viral protease automatically cleave the polyprotein into individual proteins. Additionally, positive-sense RNA undergoes a translation switch, leading to the transcription of anti-sense RNA. Meanwhile, the NS proteins that were released are directed to the replication site on ER-derived vesicle packets for transcription initiation. NS1 forms homodimers that are trafficked to the cell surface and released, resulting in secreted NS1 (sNS1). The pathway for this is unknown. (6) Nucleocapsids are formed by C proteins encasing the new viral RNA. (7) Precursor M protein (prM) and E protein embedded in the ER membrane enclose the newly formed nucleocapsid (with the help of NS1 homodimers), resulting in the formation of an immature particle. (8) Immature DENV particles are transferred to the *trans*-Golgi network. First, acidification occurs, causing conformational changes, and then the particle is exposed to furin proteases, leading to the maturation of DENV viral particles. (9) DENV viral particles are exocytosed into the extracellular matrix.[16,17] (C) Proposed visual representation of the host factors involved in the pathogenesis of dengue virus infections. Processes leading to a specific pathological event are indicated by black arrows. The green arrows indicate which events ultimately affect the endothelial cells or the hemostatic system.[16,18]

leading to clinical complications, *i.e.* coagulopathy and hypovolemic shock (dengue shock syndrome), resulting from dengue hemorrhagic fever.[19]

Infections are split into three distinct phases. Firstly, the febrile phase, lasting 2–7 d, followed by the critical phase occurring between days ~4–7. This phase begins when there is a transition from the febrile phase to the afebrile phase, known as defervescence.[14] Once the fever dissipates, commonly around day 3–7, shock, bleeding, and organ impairment may occur,[3] and although not all infections progress to the critical stage, the severity of the infection is assessed during this phase. Lastly, the convalescent phase occurs between 6–7 d after symptom onset.[8,20,21]

While these phases transpire, both virological and serological markers develop, Fig. 3.[22] During the incubation period, the viraemia increases from day 1–2, and the circulating NS1 antigen concentration increases soon after. However, the production of IgM antibodies experiences a delay, usually occur-

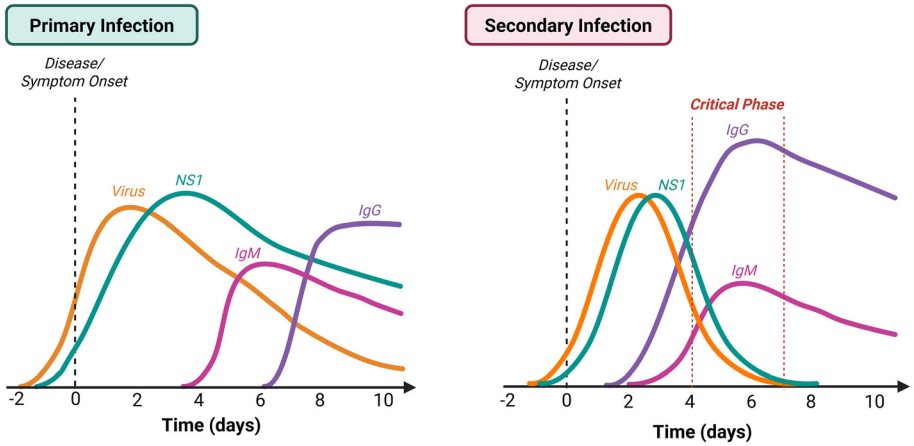

Fig. 3 Visual representation of the virological and serological markers present after infection with dengue virus according to time of illness and whether the infection of primary or secondary, created in BioRender. Etienne, R. (2025) https://BioRender.com/d7hlhh2.[22]

ring at ~day 4–5. IgG antibody production starts in the convalescent phase, and antibody levels can remain high even after the infection has cleared.[8,14] For secondary infections that do not progress into severe dengue, the infection's virological and serological markers present a different profile to primary infections, Fig. 3.

2.1 Severity of dengue infections

The risk of contracting DENV and the probability of reinfection result in varied mortality rates depending on the region.[23] Sero-epidemiological investigations indicate that second or later infections by a heterotypic DENV serotype potentially increase the risk of developing severe dengue, compared to primary or homotypic repeat infections.[1,14,24] Secondary infections are accompanied by a 2.69 times higher risk of severe dengue (SD) development.[25] This is attributable to the phenomenon of ADE.[24–26] This occurrence is owed to antiviral antibodies produced during the initial infection that occasionally circulate for a patient's lifetime. This explains the effective immunological protection against re-infection by a homotypic DENV serotype.[24] However, ADE-enhanced disease severity arises from partial immunity from a prior heterotypic infection, facilitating an improvement in DENV viral entry into Fc receptor-bearing cells.[27] Thus, ADE may result in high viral load and enhanced NS1 protein production and secretion.[19] Thus, demonstrating the importance of serotyping in dengue diagnostics. Despite the differentiation between DENV serotypes being significant for medical management, clinical screening and surveillance,[1] current RDT kits are not serotype-specific.

Infecting serotypes also pose differing severity risks. DENV-2 is considered to be the most virulent and life-threatening,[28–31] followed by DENV 4.[25,32] Both serotypes display positive correlations with severe dengue (20.6% and 20% of cases, respectively). Furthermore, the sequence of infections can be associated with a heightened risk of severe dengue development upon secondary infection. The main high-risk progression is an initial DENV-1 infection, followed by DENV-2.[33] Patients infected with DENV-1,2,4 following a previous DENV-3 infection are also at risk of increased illness severity, as demonstrated by a meta-analysis of over 15 000 DENV post-primary infection cases.[1]

3 Commercial diagnostic tests

DENV diagnosis remains essential for mitigating viral transmission and early detection for the prevention of dengue-related mortality and morbidity, especially for high-risk individuals, *e.g.* elderly patients, pregnant women, children, and patients with pre-existing health conditions.[15,20] Differentiation between Zika virus (ZIKV), DENV and Chikungunya is also of great importance as infections may present common symptoms (high fevers, myalgia, fatigue, headaches), making clinical presentation diagnoses difficult.[34–37] Additionally, accessible diagnosis eases the process of active dengue infection surveillance.[34] The format and locations where dengue diagnostic tests are performed vary depending on the timeframe and available resources. In general, there are two diagnostic avenues, molecular and immunological detection, which are mainly determined by disease stage. Followed by clinical setting/resources and geographic region.[8] Furthermore, according to the user-friendly level, these tests can be categorised as laboratory-based or RDTs for point-of-care (POC) use. WHO and the Centre for Disease Control and Prevention (CDC) have recommended the following gold standard tests: nucleic acid amplification tests (NAAT): reverse transcription polymerase chain reaction (RT-PCR), for acute (≤7 d symptom onset) DENV diagnosis, while ELISA is preferred for late acute/convalescent stages (>7 d) of infections.[8,21] Laboratory confirmations allow for a more definitive diagnosis.

3.1 Laboratory-based tests

3.1.1 Nucleic acid tests. Circulating viral components can be biomarkers, directly indicating the virus's presence in a patient. Either viral RNA genomes or proteins (antigens, see

the next section) may be screened for this purpose.[2] DENV viral RNA circulating loads are commonly found to be between 10^3 to 10^{10} RNA copies per mL.[33] On day 1 following symptom onset, the viral load is averaged at $\sim 7.24 \times 10^9$ RNA copies per mL, this value tapers off gradually throughout an infection.[38,39] The high sensitivity of DENV RNA detection *via* real-time RT-PCR (rt RT-PCR) provides a confirmatory test,[2,3] and is also accompanied by a considerably short time to results/diagnosis for a highly intensive laboratory test (usually same-day or next-day).[40] A "singleplex" rt RT-PCR assay can detect a singular serotype of DENV or all serotypes without distinguishing between them by targeting a conserved sequence. In contrast, a "multiplex" assay has the potential to detect and distinguish all four DENV serotypes. Therefore, they are advantageous for pathogenesis studies and DENV viral titre determination. The single-step multiplex real-time RT-PCR is the gold standard of DENV NAAT diagnosis.[8,40–42]

Despite the heavy presence of newly developed real-time RT-PCR methods, only two NAAT assays have FDA approval; (1) CDC DENV-1–4 real-time RT-PCR for the detection and serotyping of DENV infections in serum and plasma, with a LOD of 1×10^3 PFU mL^{-1}. (2) Trioplex rt RT-PCR assay is only employed when the risk of Chikungunya virus (CHIKV) and ZIKV infection is high. Additionally, (2) possesses a LOD of 6–15 copies per reaction for dengue detection, and the acceptable specimens are broader, including whole blood, serum, plasma, and cerebrospinal fluid.[40,42] PCR's cost and intensive processes brought about the development of PCR mimics, isothermal amplification and loop-mediated amplification methods. POCKIT and POCKIT Micro Plus, developed by GeneReach Biotech (Taichung, Taiwan),[43,44] demonstrate desirable sensitivities and specificities while maintaining one specific temperature.[8,41] The nature of these portable, small, compact devices minimises human error and allows for field diagnosis and POC testing.[43,44]

3.1.2 Antigen and serological detection

3.1.2.1 NS1 and envelope proteins. Typical laboratory-based tests are a form of ELISA, usually an antigen-capture sandwich ELISA. NS1 is a 46–55 kDa glycoprotein involved in early viral RNA replication of the DENV viral cells, maintaining diverse functionality during the viral lifecycle.[27,45,46] Secreted NS1 (sNS1) is a soluble hexameric structure, responsible for high NS1 concentrations in the infected individuals' circulatory systems.[46] sNS1 also activates the innate immune system response of infected individuals, and NS1 antigenemia levels are significantly higher in severe dengue patients.[47]

Antigenemia is heavily dependent on primary or secondary infections. The concentration range of circulating NS1 antigens is commonly quoted as 0.04–2 μg mL^{-1} and 0.01 to 2 μg mL^{-1} for primary and post-primary infections, respectively.[48] Recently, Allonso *et al.* documented 0.007 μg mL^{-1} as the lowest NS1 circulating concentration detected in their study.[49] During primary infections, NS1 antigens can remain detectable for up to 9 d following symptom onset. A positive NS1 test confirms a DENV infection, while a negative result does not eliminate an infection.[40] The majority of dengue RDTs for NS1 enlist multiple serotype-specific anti-NS1 monoclonal antibodies to enable the capture and detection of soluble secreted NS1 antigen (ssNS1) in serum, plasma, or whole blood specimens. Three NS1 ELISA tests are recurrently mentioned in evaluation-based articles: Platelia Dengue NS1 Ag ELISA (BioRad), DENV Detect NS1 ELISA (InBios International), and Panbio Dengue Early ELISA (2nd generation (Alere)).[42] An apparent limitation of NS1 detection accompanies patients experiencing post-primary infections. Lowered NS1 circulating levels resulting from a rapid anamnestic rise in antibodies for DENV NS1 neutralisation during the acute phase cause an unwanted hurdle by rapidly sequestering the antigens in immunocomplexes. Therefore, the biomarker is no longer available for detection. Inevitably, NS1 antigenemia kinetics in post-primary infections generate a shorter detection window.[8,50] An analytical reactivity study evaluating the LOD of a DENV NS1 Ag ELISA developed by Lai, S. C., *et al.*,[51] compared to Platelia's Dengue NS1 ELISA, demonstrated LOD variations between the four DENV serotypes, see Table 1.[51]

Typically, DENV NS1 is the diagnostic target; however, recently, the use of DENV envelope proteins (E-proteins) has gained traction. These antigens are present throughout the body during infection, namely the lungs, liver, leukocytes, and, most importantly, peripheral blood.[11]

3.1.2.2 IgG and IgM antibodies. Immunoglobulin proteins, Ig (M, G, E, A, and D), specific to viral antigens, are produced as a response to viral infection.[52] Both MAC-ELISA and IgG ELISA mobilise anti-IgM or IgG monoclonal antibodies and recombinant DENV-derived antigens for capture and detection by indirect conjugation of the detection element to an enzyme that initiates colour changes in an initially non-coloured substrate.[42] Additionally, a large proportion of antigens present in DENV ELISAs originate from the dengue viral envelope protein.[41,53] The most prevalent commercial ELISAs are from Standard Diagnostics (Seoul, South Korea), Panbio Inc (Alere, Waltham, WA, USA), alongside BioRad (Marnes-la-Coquette, France) and InBios International.[42,54–59] Despite this, one major complication in dengue-endemic regions is the persistence of raised IgG and IgM titres from previous infections.[58]

IgM antibody detection: IgM-based immunoassays vary in sensitivity and specificity, due to the immobilised antigen type and its quality. Regarding general commercial DENV ELISAs, all four DENV serotype E-proteins (or NS1 proteins) are included, ensuring efficient diagnosis regardless of the infecting serotype.[11,14] Thus, results from IgM detection are con-

Table 1 Detection limits of ELISA developed by S.C. Lai *et al.* for DENV NS1 and Platelia Dengue NS1 Ag ELISA.[51] Serotyping was initially confirmed with RT-PCR

	Minimum detectable concentration (ng ml^{-1}) of NS1			
NS1 detection assay	DENV1	DENV2	DENV3	DENV4
ELISA for DENV NS1	1.953	3.906	3.906	0.977
Platelia Dengue NS1 Ag ELISA	3.906	31.250	0.977	7.813

siderably reliable if the specimen collected has a low risk of other flavivirus infections.[41,53] Cross-reactivity among the flaviviruses' IgMs may lead to false positives.[53,60,61] Therefore, patients at risk of Zika, Yellow Fever (YFV), West Nile (WNV) and Japanese Encephalitis (JEV) viral infections require a combination of serologic and molecular testing.

IgG antibody detection: IgG detection may aid in differentiating primary from secondary infections. In paired sera analysis following IgG seroconversion, there's approximately a four-fold increase in the IgG titre from the initial sample.[42,62,63] Persistent, heightened IgG levels may result in unwanted inconclusive results or false positives.[42]

However, the potential lifelong presence of IgG antibodies doesn't hinder diagnostics if a spike in IgG titres can be identified using paired sera.[42] For IgG detection, commonly mentioned DENV ELISAs include DENV Detect IgG ELISA (InBios International, Inc.); Anti-Dengue virus IgG Human ELISA (Abcam); and Anti-Dengue virus ELISA (IgG) (Euroimmun). Their reported sensitivities are above 94.0%, according to Lee *et al.*, in their 2019 evaluation of six commercially used dengue diagnostic tests.[54]

IgM/IgG ratio-based testing: Comparison of IgM to IgG titre can serve as an indicator of the stage and primary or post-primary status of DENV infections.[42] A study combined an in-house IgM and IgG ELISA with the Panbio anti-dengue indirect IgG ELISA to validate the detectable difference between primary and secondary acute infections, using plaque reduction neutralization tests (PRNT) as the control standard.[64] Panbio's indirect IgG model provided the best performance in an acute infection, while the IgM/IgG ratio models were more advantageous in the later convalescent phase of infections. In combination with NS1 detection, the influence of primary and secondary infections on IgG/IgM combined testing is reduced due to the synergy between the testing results.[64]

3.2 Rapid diagnostic tests

Lateral flow tests (LFTs), the most popular form of RDT, are low-cost, simple devices requiring no training or specified skills. The most prominent labelling elements are NPs, varying from colloidal gold, carbon black, coloured polystyrene beads, quantum dots, and lanthanide-doped phosphors. Gold NPs (AuNPs) are the most popular label for commercially available tests.[1] For dengue diagnostics, LFAs suffer from low accuracy and sensitivity limitations (48–90%).[1] There are no FDA-approved DENV NS1-based RDTs. However, four popular commercial DENV NS1 RDT options include NS1 Ag STRIP (BioRad, Marnes-la-Coquette, France), Dengue NS1 Detect Rapid Test (InBios International), SD Bioline Dengue NS1 Ag Rapid Test (Abbott, Abbott Park, IL, USA), and Panbio Dengue Early Rapid (Alere, Waltham, WA, USA).[42] And because of the importance IgM detection plays in late acute and convalescent phase infections, rapid IgM-based tests are available in differing formats; LFTs and particle agglutination assays.[65] IgG incorporation offers a more complete testing profile; therefore, testing formats that detect NS1 *via* one strip, while a second strip can detect both IgM and IgG, were developed. It provides detection for different infection phases, in conjunction with improved performance.[13,58] All of the current commercial LFA kits are singleplex, and the sensitivities of the LFAs could be improved upon by the inauguration of a tapered nitrocellulose (NC) membrane for LFTs, or directional conjugation for enhanced signal.[59]

3.2.1 Dengue LFT sensitivities and specificities. A metadata study by Macêdo *et al.* assessing the sensitivities and specificities of commercially available DENV LFTs detecting lone NS1, IgG, IgM, or combinations provided a conclusive overview of the current state of RDTs and highlighted opportunities for improvement.[13] One novel non-commercial RDT and 20 other commercial brands were included, and each scientific article implemented mainly ELISA (NS1, IgM or IgG) or RT-PCR for the reference tests. From Table 2, the averaged sensitivities and specificities across all 21 brands are demonstrated. The averaged data for lone IgM and IgG-based diagnosis indicate low sensitivities, whereas the inclusion of NS1 detection to both or collectively testing for all three analytes significantly improves the sensitivity, as seen with the IgM/IgG ELISA. SD Dengue Duo kit (Standard Diagnostics, Korea) is stipulated to be the most used and the highest performing RDT, demonstrating high sensitivity for NS1 and IgM detection. The specificities for all RDTs were mostly above 90%, except for the NS1 + IgM combined RDTs. The analyte combination slightly increases the overall combined possibility of cross-reactivity.[13]

Other factors impacting LFTs' clinical and analytical sensitivities are lowered antigenemia and infecting serotype. Haider *et al*. present this by the evaluation of nine NS1-based RDTs in combination with five IgM-based tests. With cumulative sensitivities of 83.63%, testing was most sensitive to DENV-3, followed by DENV-1 (81.3%), DENV-2 (75.22%) and lastly DENV-4 (62.06%).[66] The averaged data for lone IgM and IgG-based diagnosis indicate low sensitivities. In contrast, the inclusion of NS1 detection to both or collectively testing for all three analytes, again, significantly improves the sensitivity.

3.2.2 Antigenemia *vs.* the LOD of commercial dengue LFAs. Among the documented circulating NS1 titres (antigenemia) for DENV-positive patients, a fraction is divided into primary and post-primary infections. Despite this, the overall lowest NS1 titre, or below, should remain the LOD target for

Table 2 Average sensitivities and specificities associated with commercially available LFTs for DENV NS1, IgM and IgG detection were compared with ELISA/RT-PCR as a reference. Metadata were collected and analysed by Macedo *et al.*[13]

	Averaged sensitivity		Averaged specificity	
Analyte	ELISA	RT-PCR	ELISA	RT-PCR
NS1	77%	61%	98%	93%
IgM	49%	50%	91%	98%
IgG	58%	67%	98%	94%
NS1 + IgM	72%	83%	89%	83%
NS1 + IgM + IgG	77%–99%	n/a	n/a	n/a

RDTs. Commercial LFAs advertise high sensitivity and low detection limits, yet struggle with 'in-field' sensitivities, Fig. 4.[51,67–69] On further inspection, regional clinical studies assessing commercial diagnostic sensitivities indicate that a fraction of the clinical samples presented lower NS1 concentrations than 0.04 to 2 μg mL^{-1}.[48] An inclusive updated average circulating NS1 concentration range of 0.0048–4 μg mL^{-1} could indicate the ideal LOD benchmark for advances in dengue NS1-based diagnostics[48,49,70–73] In some cases, detection limits for the developed DENV diagnostics require more stringent clarification of the LODs related to specific specimens (blood, serum or plasma) if they differ. Clinical sensitivity is influenced by a multitude of factors, one of them being specimen type, therefore, this should be considered when developing new dengue diagnostics.[55,61,74]

4 Nanoparticle-based optical biosensors

Nanosensors can generally be categorised based on the type of detection system they use, such as optical, electrical, thermal, or magnetic biosensors, see Fig. 5.[75,76] This section provides an overview of nanoparticle-based optical biosensors for dengue diagnosis, focusing on the materials used, the affinity ligands involved (such as antibodies, aptamers, and enzymes), and the optical sensor designs. Recently published reviews on DENV diagnostics are summarised in Table 3, indicating the nanomaterial employed, where applicable. Unfortunately, the majority of the NS1-based examples below, with LODs competitive enough to cover low antigenemia concentrations, would not be considered affordable and POC applicable. Moreover, the WHO published an invitation for novel dengue diagnostics in 2024. With various viable target analytes (NS1 antigens, dengue genetic material, IgM and IgG) for either molecular and serological assays or dengue multi-analyte RDTs. Each candidate's performance would be evaluated by their detection

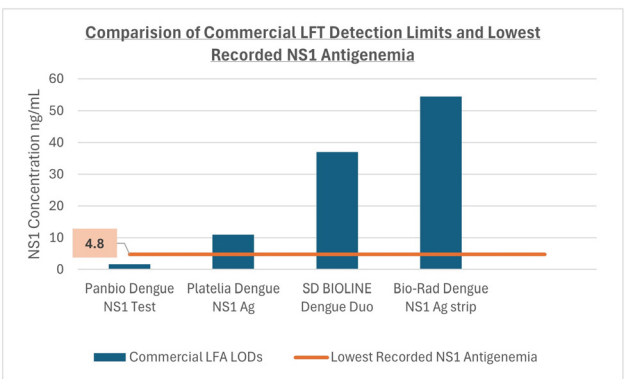

Fig. 4 Graph documenting the LODs of the popular NS1 RDTs (B), from lowest to highest detectable concentration of NS1 antigens by the LFT: Panbio (1.73 ng mL^{-1}), Platelia Dengue NS1 Ag (10.99 ng mL^{-1}), SD BIOLINE Dengue Duo (37.00 ng mL^{-1}), Bio-Rad Dengue NS1 Ag Strip (54.43 ng mL^{-1}).[50,67–69]

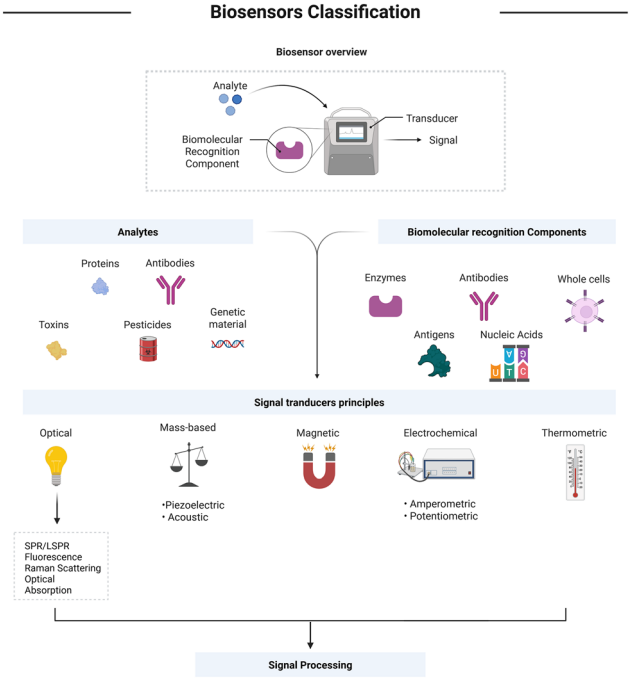

Fig. 5 Graphical representation of the components included in an optical biosensor: a sensing unit, a signal transducing unit, followed by a processing unit, created in BioRender. Etienne, R. (2025) https://BioRender.com/itw6yy0. Adapted from Chen *et al.*[76]

of recent and currently circulating dengue viruses globally. The RDTs must detect both NS1 antigens and IgM, whereas an NAAT would need to focus on acute DENV diagnosis and could be serospecific as well as pan-specific. However, POC, primary healthcare and laboratory-based settings are all applicable formats. Both RDTs and NAATs must efficiently detect all four serotypes and possess whole blood sample analysis capabilities to be POC applicable. In addition to this, WHO formally outlined the acronym 'ASSURED' (Affordable, Sensitive, Specific, User-friendly, Rapid, and Equipment free, Deliverable to end-users), now 'REASSURED' (Real-time connectivity, Ease of specimen collection, Affordable, Sensitive, Specific, User-friendly, Rapid and robust, Equipment-free/Environmentally friendly, Deliverable to end-users) for the criteria of an ideal RDT.[77] Therefore, providing a comprehensive criterion for an ideal DENV test, *e.g.* whole blood sample and POC applicable, >30 min assay run time, detects both NS1 and IgM (and, if possible IgG) for all serotypes, but serotyping isn't required.[6,78,79]

4.1 DENV-specific biological diagnostic components

Molecular recognition of the target analyte by the bioreceptor is paramount for detection. Laboratory-synthesised bioreceptors have been widely implemented over recent years and are usually coined to elicit high selectivity for the desired target. Frequently used bioreceptors include: antibodies, nucleic acids (DNA/RNA), aptamers, whole-cell and enzymes.[111] The majority of DENV biosensors fall under the category of

Table 3 Summary of recently dengue diagnostics and their corresponding analytes[10–12]

No.	Analyte	Detection method	LOD	Concentration range	Nanomaterial (if applicable)	Ref.
1	NS1	DPV	6.8 ng mL^{-1}	20–800 ng mL^{-1}	Carbon nanotubes	80 and 11
2	NS1	DPV	3 mg mL^{-1}	10^{-12}–10^{-6} g mL^{-1}	AuNPs	11 and 81
3	NS1	EIS	0.3 ng mL^{-1}	1–200 ng mL^{-1}	—	10, 11 and 82
4	NS1	ECS	3.0 ng mL^{-1}	10–2000 ng mL^{-1}	—	11 and 83
5	NS1	CV	0.1 ng mL^{-1}	1–100 ng mL^{-1}	—	11 and 84
6	NS1	SPW	5.73 pg mm^{-2}	—	—	12 and 85
7	NS1	LSPR	1.54 nM	—	AuNPs	12 and 86
8	NS1	SERS	15 ng mL^{-1}	15–500 ng mL^{-1}	—	12 and 87
9	NS1	Colourimetric	DENV-1 = 1.4 ng mL^{-1} DENV-2 = 0.7 ng mL^{-1} DENV-3 = 1.4 ng mL^{-1} DENV-4 = 6.6 ng mL^{-1}		Magnetic nanoparticles – carboxyl-adembeads	10 and 88
10	NS1	Fluorescence	15 ng mL^{-1}	15–500 ng mL^{-1}	–	10 and 89
11	NS1	EIS	340 pg mL^{-1}	1–5000 ng mL^{-1}	–	10 and 90
12	NS1	EIS	1.67 ng mL^{-1} (standard); 1.19 ng mL^{-1} (spiked)	—	Langmuir–Blodgett (LB) films of molybdenum disulphide (MoS_2) and AuNPs	10 and 91
13	NS1	DPV/EIS	1.49 μg mL^{-1}	—	—	10 and 92
14	IgG	EIS	2.81 ng mL^{-1}	62.5–2000 ng mL^{-1}	Graphene/titanium dioxide (G/TiO_2) nanocomposites	11 and 93
15	IgG	EIS	22.5 ng mL^{-1}	125–2000 ng mL^{-1}	G/TiO_2 nanocomposites	11 and 93
16	IgG	EIS	6100 pg mL^{-1}	10–1000 ng mL^{-1}	—	10 and 90
17	ssDNA	CV	43 μM	10^{-6}–10^{-4} M	Zinc oxide/platinum-palladium (ZnO/Pt–Pd) nanocomposites	
18	DNA	LSPR	1 fM	10^{-15}–10^{-10} M	Quantum dots and AuNPs	11 and 94
19	DNA	FORS	1 zM	10^{-21}–10^{-12} M	Gold latex spheres	11 and 95
20	DNA	SERS	0.49 fM	10^{-15}–10^{-9} M	AgNRs	11 and 96
21	DNA	DPV	9.4 fM	10^{-14}–10^{-6} M	AuNPs and nitrogen, sulfur codoped graphene quantum dots nanocomposite (N, S-GQDs)	10, 11 and 97
22	DNA	Colourimetric	0.2 aM	10^{-16}–10^{-10} M	Silica nanospheres	12 and 98
23	DNA	Reflectometric	1 zM	10^{-15} M–10^{-11} M	Silica nanoparticles	12 and 99
24	DNA	FET	2.0 fM	10^{-15}–10^{-6} M	Silicon nanowires (SiNWs)	10 and 100
25	DNA	LSPR	DENV-1 = 24.6 fM DENV-2 = 11.4 fM DENV-3 = 39.8 fM DENV-4 = 39.7 fM	10^{-15} to 10^{-10} M	Cadmium selenide tellurium sulphide fluorescent quantum dots (CdSe/TeS QDs) and AuNPs	10 and 94
26	DNA	DPV/CV	1.63×10^{-12} M	10^{-11}–10^{-7} M	SiNWs and AuNPs	10, 12 and 101
27	RNA	EIS	20 PFU mL^{-1}	10^{2}–10^{5} PFU mL^{-1}	—	11 and 102
28	RNA	Colourimetric	—	—	AgNPs	12 and 103
29	RNA	Colourimetric	1.2×10^{4} pfu mL^{-1}	0.01–0.06 μM	AuNPs	10 and 104
30	E-proteins	SPR	0.1 pM	10^{-13}–10^{-10} M	Gold/cadmium sulfide quantum dots	11 and 105
31	E-proteins	TOF	1.0 pM	10^{-13}–10^{-6} M	Polyamidoamine (PAMAM)	11 and 106
32	E-proteins	TOF	1.0 pM	—	—	11 and 107
33	E-proteins		1.0 pM	0.01–0.1 nM	Amine functionalised graphene oxide composited cadmium sulfide quantum dots ($CdS\text{-}NH_2GO$)	10 and 108
34	Nucleic Acids	SPR	31–260 copies per mL	—	AuNPs	12 and 109
35	DENV virus particles	SRP	2×10^{4} particles per ml	—	—	10, 12 and 110

Abbreviations: limit of detection, LOD; single stranded, ss; DPV, differential pulse voltammetry; EIS, electrochemical impedance spectroscopic; CV, cyclic voltammetry; LSPR, localised surface plasmon resonance; FORS, fibre optics reflectance spectroscopy; SERS, surface-enhanced Raman spectroscopy; SPR, surface plasmon resonance; AuNP, gold nanoparticles; AgNRs, silver nanorod; TOF, tapered optical fibre; SPW, surface plasmon waveguides; FET, field effect transistors.

"affinity biosensors". Antibodies, aptamers, and nucleic acids are used for DENV analyte detection; therefore, the target analyte is bound to the receptor irreversibly. The alternate class of "catalytic biosensors" includes enzymes, whole cells, tissues, and microorganisms. For this class, the interaction between the target and the receptor induces the production of a biochemical product.[75] The major challenge dengue bioreceptors face is the required genetic diversity to detect pan-DENV infections, covering serotypes 1–4, while also excluding unwanted detection of infections for ZIKA and other flaviviruses.

4.1.1 Aptamers alternative to antibodies. Antibodies (Abs) are the recognition components in the majority of dengue diagnostics, followed by RNA/DNA. More recently, both monoclonal and polyclonal antibodies (mAbs and pAbs) have been produced on large scales due to their recurring inclusion into diagnostics.[112] Commonly, these antibodies are sourced from host species like mice, goats and humans. Recombinant mAbs are favoured in dengue diagnostics, especially for high selectivity. Three categories are usually present in antibody-based testing: capture antibodies, detection antibodies and control antibodies. Detection Abs are labelled and bind specifically to the analyte, whereas capture Abs are immobilised. The desired characteristic for capture Abs is high. Specificity, however, is heavily influenced by the detection antibodies. These require both high specificity and sensitivity, while also providing a strong signal when bound.[113] Despite their advantages, their limitations may include limited shelf life, pH sensitivity, and irreversible denaturation, which narrows the effectiveness of these antibodies.[114,115] Aptamer incorporation as a recognition component for proteomics and clinical diagnostics has been documented for years and is becoming increasingly visible in dengue diagnostics. Aptamers (Apt), discovered by Gold *et al.* and Szostak *et al.*, are manufactured oligonucleotides, predominantly between 10–100 nucleotides.[115–117] They're either single-stranded RNA or DNA (ssRNA/ssDNA), able to bind to specified targets.[118] These nucleic acid sequences are deemed antibody equivalents but present characteristically low immunogenicity, providing an advantage over antibodies for combating clinical sensitivity.[115] Aptamers are routinely selected *via* Systematic Evolution of Ligands by Exponential Enrichment, *i.e.* SELEX, composed of 4 steps: pool generation, selection, amplification, and isolation.[112,119–122] DNA-based sequences bring forth more diverse, stable aptamers. A prominent advantage of aptamers is that their 3D structures can be manipulated chemically and/or labelled with differing functional groups and probes without impacting the binding interactions. Moreover, aptamers demonstrate reversible thermal denaturation, alternative buffer stability and long storage capabilities.[114,115] Incorporating aptamers into colourimetric sensing, creating optical biosensors for UV-Vis or naked eye detection, are among the simpler designs for aptasensors. Thus, providing a favourable alternative avenue for the improvement of dengue LFTs. Categories of aptamer biosensors are as follows: colourimetric aptasensors, horseradish peroxidase (HRP)-mimicking DNAzyme aptasensors, fluorescence aptasensors, electrical aptasensors, and label-free aptasensors.[114,115] Incorporation of aptamers into nanosensors may result in sensitivity improvement or provide a route for signal amplification, despite the potential limits resulting from sterically driven 1 : 1 aptamers-target binding. Aptasensors' contributions to POC DENV diagnostics have recently been explored, as indicated by Table 4.

4.1.2 Enzyme-based nucleic acid sensors. Biocatalysts (enzymes), increase the biological rate of reaction. Consequently, sensors usually rely upon the enzyme's ability to bind to the desired target,[75] and are divided into two categories: (1) Catalytic biosensors, where interactions with the target produce a new biochemical product. (2) Affinity biosensors; the analyte binds to the transducer surface.[133] Recognition mechanisms are categorised into three of the following: (a) catalytic analyte transformation measurements resulting from enzyme metabolization, allowing enzyme concentration analysis. (b) Activation or inhibition of the enzyme by the desired analyte, where higher analyte concentrations are directly proportional to the decrease in enzymatic product formation. (c) Enzyme structure alteration tracking.[75] Enzyme-based sensor limitations include: low diagnostic sensitivity, sensitive structures, high costs, the need for improvements to enzyme stability, and their adaptability is restricted and complicated.[75,134] Currently, ELISA is the main example of enzymatic DENV diagnosis. Despite this, inhibitory aptamer restriction endonuclease complex incorporation can underpin signal transduction for a fluorescence-based biosensor. Fletcher *et al.* presented an oligonucleotide with the ability to form stem/loops employed for DENV nucleic acid detection.[135] The advantage of restriction endonucleases is their high speed, efficiency, and specific cleavage of nucleic acid substrates. Their customisability influenced whether it fits the desired signal detection model. Pan-DENV, as well as singular serotype detection, was demonstrated with their biosensor in a reproducible manner with high specificity. Heterologous regions discovered in the DENV-1–4 genomes produced serospecific linkers, while a homologous genome sequence allowed for pan-DENV detection. Restriction endonuclease (EcoRI), demonstrates inhibited activity when bound to the detection aptamer. However, in the presence of the trigger oligonucleotide sequences, the EcoRI enzyme is rapidly released from its previous Apt_EcoRI complex. The now free EcoRI enzyme cleaves a modified molecular break-light (MBL).[136] Much like the detection aptamer, the MBL is a stem/loop-forming oligonucleotide sequence in the possession of both a 5′ fluorophore and a 3′ quencher. In turn, cleavage of the 5′ fluorophore from the 3′ quencher produces a detectable signal proportional to the concentration of free EcoRI enzyme.[135] The theme of pairing oligonucleotides with complementary cleavage enzymes for fluorescent DENV serotyping was further expanded on by the integration of nanostructures. Chan *et al.* proposed serotyping dengue-infected mosquitoes by presenting a label-free silver nanocluster (AgNC)-based DNA biosensor.[137] DNA polymerase and a 'nicking enzyme' (Nt.BstNBI) were enlisted for DENV detection by an isothermal amplifica-

Table 4 Examples of DNA and RNA aptamer-based dengue diagnostics. Abbrev. PBS, phosphate-buffered saline; BSA, bovine serum albumin

No.	Sequence	Detection principle	Serogroup and target protein	DNA or RNA aptamer	LOD	Equilibrium dissociation constant (K_d)	Negative control	Ref.
1	5′-HS$(CH_2)_6$ – TTTTT – ACTAGGTTGCAGGGGACTGCTCGGGAT TGCGGATCAACCTAGTTGCT TCTCTCGTATGAT-3′	EIS	DENV-1 and DENV-4 NS1 protein (in PBS and human serum)	DNA	0.05 ng mL^{-1} (PBS + BSA (0.1%) buffer solution) 0.02 ng mL^{-1} (undiluted serum)	n/a	DENV E-protein	123 and 124
		ECS	DENV-4 NS1 protein	DNA	30.9 fg mL^{-1} (PBS) 41.8 fg mL^{-1} (undiluted serum)	n/a	1 ng mL^{-1} E protein in undiluted serum	125
2	Aptamer (TDENV-3) 5′-GGCCTTCACTGCTTTGATCTCGTGGGGGTGTGTCGCGG GAGACACCATGGAATATATGGCC-3′ Aptamer (TDENV-6a) 5′-TCTAATACGACTCACTATAGCCGTAGTCGTATCTCCATTACCC AGAATGGTGATGCGCCG-3′	ELASA	RNA Aptamer for DENV-2 NS1 protein	RNA	NS1 spiked human serum 12.5 nM (TDENV-3) 25 nM (TDENV-6a)	DENV-3 = 37.57 ± 10.34 nM DENV-6a = 41.40 ± 9.29 nM	0 nM NS1 in human serum (LOD) 3 control sequences against DENV-2 NS1 were used to assess binding affinities	126
3	5′-SH/- CCCGCACCGGGCAGGACGTCCGGGGTCCTCGGGGGGCGGG-3′	Colorimetric	DENV-1–4 ED3[a]; DENV 1–4 Plaque neutralization assay	DNA	Mixed DENV-1–4 pool = 10^6 $TCID_{50}$	DENV-2-ED3 = 200 nM	SAMNs@MPA	127 and 128
		Fluorescence			Human serum = 1 × 102 pfu mL^{-1} Plasma = 1 × 103 pfu mL^{-1}		Hexagon-centred star sensor (sensor positive control) (LOD of 1 × 103 pfu mL^{-1}) Inhibitor free plaque well (plaque reduction control)	128 and 129
4	5′- CGGCATTCTCCTGCTACGAGG-CGCTGCGGTACACCCCGACTCCAC-GAGCCACTGTCTACGGACATCTG -3′	Chemiluminescence/ thermophoresis	DENV-2-EIII	DNA	n/a	154 nM	500 nM imidazole	130
5[b]	AptD1 5′-CCCCAGACGGACTGGTGTXCTCGGxATGGCC GTCTGGGGCGCGLAGCG-3′	ELISA	NS1 Proteins: DENV-1	DNA	DENV-1 NS1 1.60 ng mL^{-1} (buffer); 2.22 ng mL^{-1} (serum)	AptD1-DEN1-NS1 (K_d = 107 pM)	4 control sequences (binding affinities) Cont-D1-1-49 h: 5′-CCCCAGACGGACTGGTGTACTCGGAATGGCCGTCTGGGGC GCGLAGCG-3′ K_D = 1.3 μM	131
	AptD2 5′- GGctgGTCCGxCTGGGAACAAGxGGCGGGAGGGAdGGGTG TGGGTGCgacaagcggaCCagCCCGCGLAGCG-3′		DENV-2		DENV-2 NS1 1.86 ng mL^{-1} (buffer); 1.99 ng mL^{-1} (serum)	AptD2-DEN2-NS1 (K_d = 65 pM)	Cont-D2-1d-72 h: 5′-GGctgGTCCGACTGGG AACAAGAGGCGGGAGGGATGGGTGTGG GTGCgacaagcggaCCagCCCGCGLAGCG-3′ K_D = 104 pM	
	AptD3 5′-CCGCTTGTCATCTAxCCTGGCCxTGTGGTACTGTAAC GGCTgacaagcggCGCGLAGCG-3′		DENV-3		DENV-3 NS1 2.36 ng mL^{-1} (buffer); 3.31 ng mL^{-1} (serum)	AptD3-DEN3-NS1 (K_d = 75 pM)	Cont-D3-2-59 h: 5′-CCGCTTGTCATCTAACCTGGCCATGTGG TACTGTAACGGCTGACAAGCGGCGCGLAGC G-3′ K_D = 0.19 μM	
	AptD4 5′- CgGCGGAGACGTAACGCxTATCAAATCxAAACAGCTTAGGGT CCgCcGCGCGLAGCG-3′		DENV-4		DENV-4 NS1 1.19 ng mL^{-1} (buffer); 1.14 ng mL^{-1} (serum)	AptD4-DEN4-NS1 (K_d = 27 pM)	Cont-D3-2-59 h: 5′-CCGCTTGTCATCTAACCTGGCCATGTGG TACTGTAACGGCTGACAAGCGGCGC GLAGCG-3′ K_D = 0.19 μM Cont-D4–3–57 h: 5′ – CgGCGGAGACGTAACGCATATCAAATCA AAACAGCTTAGGGTCCgCcGCGCGLAGCG – 3′ K_D = 2.0 nM	
[b]	Same as above[a]	ELISA (competitive)	Anti-DENV human IgG antibodies	DNA	Can detect IgG antibodies in samples with volumes as low as 0.05 μL	Aptamers: K_D = 30–182 pM; Ab#D06 (detector agent): DENV-1, DENV-2, DENV-3 DENV-4: 107, 65, 75, and 27 pM, respectively	Healthy volunteers serum samples (control serum – absence of Anti-DENV IgG antibodies)	132

[a] Abbreviations: limit of detection, LOD; single stranded, ss; DPV, differential pulse voltammetry; EIS, electrochemical impedance spectroscopic; CV, cyclic voltammetry; LSPR, localised surface plasmon resonance; FORS, fibre optics reflectance spectroscopy; SERS, surface-enhanced Raman spectroscopy; SPR, surface plasmon resonance; AgNRs, silver nanorod; TOF, tapered optical fibre; SPW, surface plasmon waveguides; FET, field effect transistors. [b] The K_d values are the same as the example before, as they use the same aptamer sequence.

tion method. Serospecific DENV-1–4 DNA probes for designated regions in the target DNA sequence provide the serotyping capabilities. DENV DNA hybridises, creating a primer for Vent (*exo*-) DNA polymerase to produce a complementary strand. Whereby, oligonucleotide cleavage by Nt.BstNBI releases the target DNA and AgNC strands complementary to the probe. The repetition of this cycle subsequently results in DNA amplification and high AgNC strand concentrations. Wherein, AgNC strands react with $AgNO_3$, followed by a $NaBH_4$-led reduction, giving way to AgNC formation. Fluorescence spectroscopy allowed for AgNC visualisation between AgNC concentrations of 0.5–3 μM, quantifying the presence of the DENV target.[137]

4.2 Designs of optical nanosensors for dengue

Optical biosensors, recognised for their effectiveness as biological analyte detectors, have numerous applications: drug discovery and development, environmental monitoring, and enhancement of medical diagnostics.[11,76] They include 3 units: a sensing, signal-transducing and processing unit. Biomolecular interactions underpin the detection processes, and recognition between biomolecules occurs by affinity binding and catalysis. Affinity binding biosensors are more efficient, as analyte binding creates a detectable thermodynamic equilibrium. The advantage of optical signal detection is the signal stability as it's undisrupted by external disturbances, the method is also highly sensitive.[76]

In this section, the nanosensor designs have been classified by their operating principles. The NP components may directly lead to LSPR-based sensing, but the use of non-SPR colourimetric sensing, fluorescence, and SERS-based biosensing applications also plays a major role in the recent dengue diagnostic advances.[138,139]

4.2.1 SPR/LSPR-based nanosensors. The phenomenon, SPR, first observed in 1902, occurs on surface conducting materials, predominantly metals, when the metal-dielectric interface is subjected to polarised light of a specific angle.[140,141] Surface plasmons (SP) are the result of the interaction between photons from the incident wave and the electrons in the metal's surface.[76,140] The SPs propagate parallel to the metal's surface, resulting in the light reflected at the resonance angle experiencing a reduction in intensity.[76,140] SPs are sensitive to changes in the metal's surface, and sensograms can be produced by monitoring the shifts in reflectivity, wavelengths or angles against time. Therefore, when a ligand is immobilised on a sensor's surface, the interaction between the ligand and the target analyte can be measured. The binding and absence of binding between is indicated by the association and dissociation phases in the sensorgram.[141] The basic operating principle of SPR sensing is indicated in Fig. 6,[140,142] where the incident light is directed at the metal's surface through a prism, and reflected light experiences a drop in intensity.[141] The shift in intensity is measured by the optical detector, the sensor chip is comprised of a gold surface that has been functionalized to allow for ligand immobilisation, and the fluidics system provides a 'flow-through' pathway for

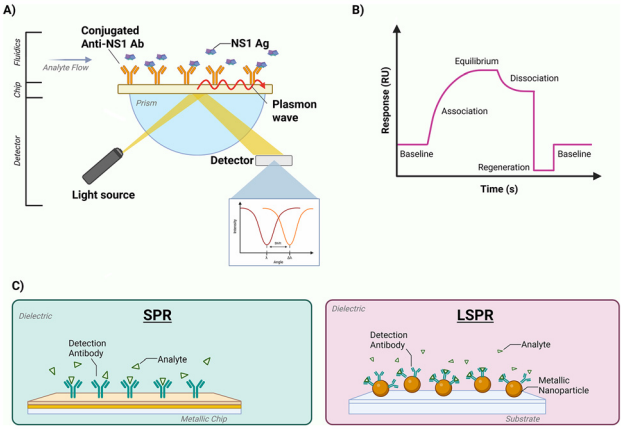

Fig. 6 (A) Schematic representation of the general principle used in SPR biosensing, including a reflectance spectra at the detector. (B) Graphical representation of a generic SPR sensorgram, highlighting the steps involved in an analytical cycle.[140,142] (C) Schematic representation of differences between SPR and LSPR biosensing principles.[147] This figure was created in BioRender. Etienne, R. (2025) https://BioRender.com/6k9p9i2.

the analyte to bind to the ligand.[140,141] The changes in the refractive index on the sensor's surface provide a real-time detection method for DENV serologic or antigen detection, as the bimolecular interactions result in the polarised light hitting the surface to experience a spectrum change due to angular shift.[42,143] BIACORE instruments, Biacore AB, are examples of evanescent wave-based instruments, where the optical detection principle is SPR. LSPR sensing arises from the optical phenomenon, LSPR, which is the product of the interaction between light and conductive NPs. The NPs' optical properties are unique and aren't present in their larger structures. When these nanoparticles are exposed to incident light, the conduction band electrons experience induced simultaneous oscillation. A charge separation occurs as the electrons oscillate around the particle's surface. Therefore, in the direction of the light's electric field, a dipole oscillation forms as a result of the equilibrium of the electron clouds being disrupted. At a specific frequency of the incident light, this oscillation can reach a maximum, which is known as SPR and light within the ultraviolet-visible band is strongly absorbed or scattered.[144,145] The SPR of bulk materials and nanoparticles differ, see Fig. 6, as the incident wavelength is larger than the particle size, producing the phenomenon, LSPR, where the surface plasmon associated with the particle oscillates locally, rather than propagating parallel to the metal-dielectric interface.[76,140,146,147] For noble metal nanoparticles, LSPR absorbance maxima occur in the visible region.[76,140] The absorption peak determined by the reflective index of the medium forms the foundation for LSPR biosensors, as they monitor the shifts in the nanoparticle's LSPR absorption peak wavelength.[76] Many factors influence LSPR, including particle composition, metal type, size, shape, surface ligands, in addition to the particles' surrounding medium and tempera-

ture, and changes to these factors can result in colour changes and absorption peak shifting.[76,140,144,145,148] Noble metal NPs have the advantage of being coloured, which is exploited in visual detection assays because they produce a cost-effective route for detection, and varying their size and shape leads to different characteristics. The NPs also have the potential to be multiplexed, used in a solution format or attached to surfaces, further demonstrating their versatility. LSPR biosensing is commonly reliant on (1) NP aggregation, (2) local refractive index changes, or (3) charge transfer interactions at the NP's surface.[149] There are a multitude of advantages of SPR/LSPR-based sensors, as indicated by Table 5.

4.2.1.1 Microfluidics. Microfluidic biosensors utilising SPR to detect dengue biomarkers were demonstrated in 2019. Austin Suthanthiraraj and Sen produced a lab-on-a-chip device by exploiting silver nanostructures' LSPR effect.[153] The silver nanostructures were assembled by the thermal annealing of thin silver metal film, providing a surface for anti-NS1 antibody immobilisation, thus, allowing DENV NS1 antigen detection, see Fig. 7. The device performs polyethersulfone membrane-based blood plasma separation from a small whole blood sample (10 μL) and the plasma is filtered out *via* gravity at the inlet channel. An additional advantage is the speed of diagnostic results, as the complete assay run time is 30 min. With a LOD of ~0.06 μg mL^{-1} for NS1 sample concentration, this device is within the clinical levels of circulating NS1 antigen concentrations, but sensitivity could be improved.[153]

Microfluidic nanosensors do not rely only on LSPR. Pan-DENV NS1 detection was proved possible by using a semi-quantitative microfluidic immuno-magnetic agglutination (IMA), ViroTrack Dengue Acute (91.9%), which rivals the sensitivity and run time of the gold standard ELISA (97.2%).[154] IMA assays are specifically applicable for the detection of biomarkers. Capture molecules (*i.e.* antibodies, ligands, nucleotides) coat the surface of magnetic NPs (MNPs), so aggregation occurs in the presence of the target analyte. ViroTrack IMA uses a mixture of anti-DENV NS1 monoclonal antibodies to coat the MNP surfaces, and the microfluidic chip requires insertion into a portable opto-magnetic reader, BluBox (BluSense Diagnostics) for analysis.[155] The sample is incubated with the antibody-coated MNPs and under strong magnetic fields, aggregation occurs due to MNP alignment, see Fig. 7. Changes to the transmitted light from the laser resulting from magnetic rotation of the aggregated MNPs indicate the presence of DENV NS1 in a sample. Notwithstanding the high sensitivity, 91.9%, for an RDT and the small sample size of 30 μL of serum, plasma or whole blood, the run time for DENV detection is only 12 min following sample loading. Therefore, it could compete with the LFTs used for POC DENV diagnosis.[154]

4.2.2 Colourimetric-based biosensors. Colourimetric-based biosensing not only involves SPR effects but also changes in optical absorption. SPR changes in peak position and bandwidth resulting from aggregation and biorecognition all form the basis of colourimetric biosensors. Colourimetric sensors largely depend on the optical properties of the dispersed or

Table 5 Advantages and disadvantages associated with SPR-based diagnostic techniques[150–152]

Advantages of SPR/LSPR sensors	Disadvantages of SPR/LSPR sensors
• High sensitivity	• Steric hindrance of bound detection structures
• Minimal sample pre-treatment	• Risk of data misinterpretation
• Minimal sample consumption	• Non-specific binding to the sensor surface
• Inexpensive	• Low selectivity
• Easily operated	• Low detection of membrane-bound species
• Real-time monitoring	• Shallow penetration depth
• Reusable	
• Naked eye detection	

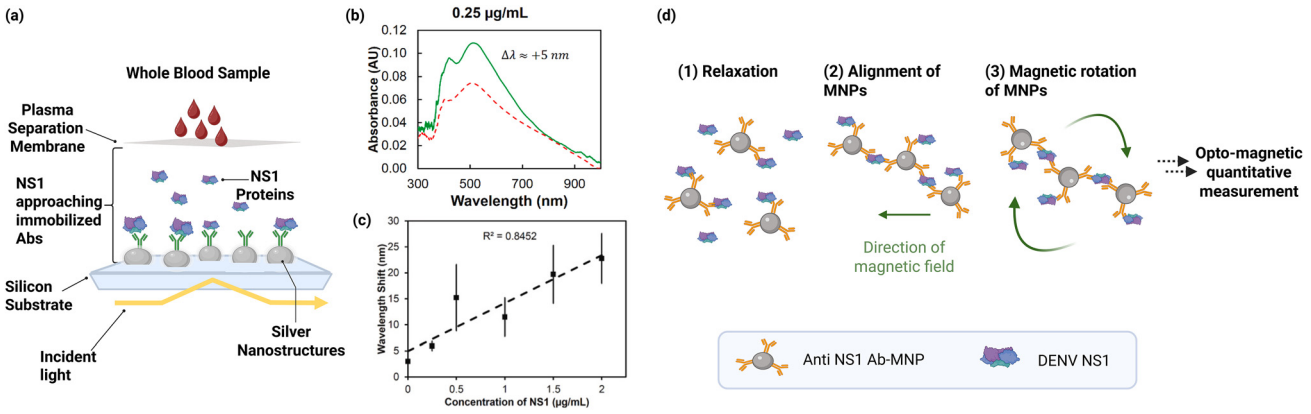

Fig. 7 (a) Visual representation of DENV NS1 lab-on-a-chip sensing region using silver nanostructures for LSPR sensing, with whole blood separation using a plasma separation membrane [reproduced and adapted with permission].[153] (b) Absorbance spectra produced from plasma incubation from whole blood sample containing 0.25 μg mL^{-1} DENV NS1 (green solid line), indicating a wavelength shift from the control absorbance (red dashed line) [reproduced with permission].[153] (c) Wavelength variation plot of whole blood sample with increasing NS1 concentrations, demonstrating linearity (R^2 = 0.84) [reproduced with permission].[153] (d) Diagram of the IMA principle used for DENV NS1 detection, using measured modulation of a transmitted laser upon magnetic field-induced rotation of the magnetic NPs [reproduced and adapted].[154] Created in BioRender. Etienne, R. (2025) https://BioRender.com/55g6mhh.

aggregated NPs, as aggregation demonstrates a colour change.[156] However, aggregation must only operate between two limiting colours, commonly red and blue.[157] Simple colourimetric detection possesses the potential for very efficient low-concentration analyte detection. Many examples of Ag/Au-based aggregation detection require acidic environments. Duyen *et al.* provided a dengue diagnostic that relies on acid-controlled aggregation of AuNPs.[38] RNA-DNA heteroduplexes form by hybridisation between DNA-functionalised AuNPs and the target DENV RNA in samples. The genetic sequence attached to the AuNPs is highly conserved in all DENV-1–4 genomic RNA, providing a method for pan-DENV detection. However, virus detection was only attempted using DENV-1 RNA. Electrostatic variations between the unbound DNA–AuNPs and the hybridised heterocomplexes form the foundation for this method's transduction principle. HCl induces AuNP aggregation in the presence of the target analyte, turning the detection solution from red to blue. Unbound single-stranded (ss) DNA–AuNPs are protected from HCl-induced aggregation as the strands provide adequate protection. Increased rigidity in the double-stranded (ds) DNA formed during hybridisation leaves the AuNPs unstable, as the ds-DNA can no longer cover the AuNP surface efficiently with its nucleobases. Therefore, the DNA's charged phosphate moieties are no longer exposed to the HCl-induced acidic environment, so aggregation occurs. The time taken for sample analysis was 1 h, and detection *via* naked eye had a LOD of ~250 pg μL^{-1} (~4.15×10^8 RNA copies), which can be improved *via* spectrophotometric analysis to 1 pg μL^{-1} (equivalent to 1.66×10^6 RNA copies), providing an attractive alternative to commonly used thermal PCR.[38]

Linares *et al*. investigated silver-enhanced AuNPs, dyed latex beads and carbon black NPs to enhance the LOD of dengue NS1 using LFTs. The sensitivity was preliminarily investigated using streptavidin and biotin to assess the best NP material. Carbon black's sensitivity dominated with a low value of 0.01 μg mL^{-1}, whereas silver-coated AuNPs presented a sensitivity of 0.1 μg mL^{-1}, while the AuNPs only achieved 1 μg mL^{-1}. This was further translated to NS1 detection; the carbon black nanosensor demonstrated a LOD of 57 ng mL^{-1} for NS1 detection, while the AuNP-based sensor was 10 times higher, with 575 ng mL^{-1}.[158] Following on from this, Yrad *et al.* proposed a DENV-1 RNA LFT with dextrin-capped AuNPs as labels, and sandwich-type hybridisation of nucleic acids formed the basis of the assay. A DENV-1-specific DNA probe immobilised on an NC membrane captured the DENV-1 RNA target, and the DNA-labelled AuNP reporter probe can confirm target detection. 1.2×10^4 pfu mL^{-1} was the lowest detectable concentration of DENV-1 RNA in pooled human sera.[104]

Due to the importance of serotyping dengue infections, Lai *et al.* developed a low-cost diagnostic for detecting and serotyping DENV NS1 antigens.[68] Their LFT format accomplished serotyping by the use of cross-reactive anti-NS1 monoclonal antibodies and serospecific monoclonal antibodies for the detection, capture and differentiation between each serotype. The LFT incorporated AuNP labels and had a run-time of 15 min. The sensitivity and specificity were determined using ELISA pre-validated serum samples, and virus culture supernatants from Japanese Encephalitis virus (JEV), ZIKA, West Nile virus (WNV), Yellow Fever virus (YFV), and CHIKV. The test exhibited no cross-reactivity with other flavivirus-infected samples. The serotyping was carried out over two different test strips: (1) DENV-1 and 4 detection, and (2) DENV-2 and 3 detection, using RT-PCR as a reference technique. The LOD for each dengue serotype were 31.25 ng mL^{-1} for DENV-1, DENV-2, DENV-4 and 15.625 ng mL^{-1} for DENV-3. Moreover, the sensitivities for their LFT strips with regard to each serotype were DENV-1 (90%), DENV-2 (88.24%), DENV-3 (82.61%), and finally DENV-4 (83.33%). The sensitivities are relatively high; however, the sample pool was small and may not be a true representation of the LFT's performance. Negative samples were cross-checked *via* RT-PCR, DENV IgM/IgG capture ELISA, in addition to dengue NS1 antigen capture ELISA. All serotype specificities were above 95%, DENV-1 (98.74%), DENV-2 (96.13%), DENV-3 (99.39%), DENV-4 (97.04%) and possessed an accuracy of above 90% (97.35%, 94.71%, 97.33%, and 95.72% for DENV-1, DENV-2, DENV-3 and DENV-4, respectively). The results from this test strip are promising, but the LOD and analytical sensitivities could undergo optimisation to enhance the test's diagnostic abilities.[68]

To combat the disadvantages of commercial PCR testing, Jiang *et al.* developed a plasmonic photothermal (PPT)-reverse transcription-colourimetric polymerase chain reaction (RT-cPCR) test. It is a simplified PCR platform centred on the photocatalytic characteristics of double-stranded DNA-SYBR Green I dye (dsDNA-SGI) complexes and plasmonic magnetic nanoparticles (PMNs).[159] The PMNs are exploited as homogeneous nano-sized heaters. After PPT-based RNA amplification, the diagnostic solution undergoes a colour change from colourless to blue in the presence of the analyte.[159] This colour change is visible to the naked eye and results from blue LED illumination-triggered oxidation of 3,3′,5,5′-tetramethylbenzidine (TMB). Without DENV RNA present, dsDNA-SGI complexes do not form, TMB is not oxidised, and the solution remains colourless. The run-time for this method was ~54 min, with a LOD of 1.6 copies per μL of DENV-2 RNA.[159]

4.2.3 Fluorescence-based. Fluorescence is a form of short-lived luminescence, where the absorbance of electromagnetic radiation by a molecule gives rise to the emission of light.[160,161] By subjecting a fluorescent molecule (fluorophore) to light (photons) of a specific wavelength, the excitation from photon absorption results in an electron transfer into the singlet state and the light emitted from the molecule is of a longer wavelength (Stokes shift), see Fig. 8.[162] Moreover, there is only a short time interval of approximately 10^{-9} seconds between absorption and emission of light.[160,161] Fluorescence-based biosensors are commonly single-fluorophore assays or two-fluorophore assays. For example, direct labelling of the target analyte with fluorescent dye, proximity assays, and Förster resonance energy transfer (FRET).[160] In a potential single fluorophore assay, binding between the target and a labelled ligand results in a change in the fluorophore's

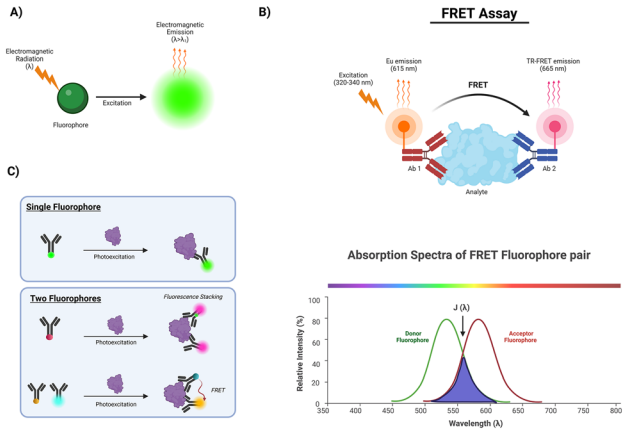

Fig. 8 (A) Visual representation of the excitation of a fluorophore leading to fluorescence (electromagnetic radiation emission). (B) Illustration of a typical FRET assay and an absorption spectra of a donor and acceptor fluorophore pair in FRET, with the overlap indicated by $J(\lambda)$.[161] (C) Schematics for fluorescent protein-based biosensors. Single-fluorophore: interaction between antibody and target changes the fluorophore's environment. Two-fluorophore based biosensors: Stacking of two identical fluorophores or using two different fluorophores, and FRET is recorded.[161] Created in BioRender. Etienne, R. (2025) https://BioRender.com/yqokze2.

environment, producing a detectable change in fluorescence intensity (Fig. 8).[161] Factors that can influence the fluorophores' environment are protein interactions, polarity and solvent changes.[161] Whereas, in a proximity assay, the target analyte binding reduces the distance between two separate fluorophores, leading to changes in the fluorescence intensity, and this method does not require direct labelling but an optimised probe.[161] FRET is also incredibly sensitive to changes in distances between two fluorophores, as this method is reliant on the energy transfer between adjacent fluorophores (acceptor and donors).[161,162] The acceptor undergoes direct excitation due to the energy transferred from the donor fluorophore, and light of a specific wavelength then excites the donor. Thus, FRET requires compatible fluorophore pairs and is preferred when investigating conformational changes and molecular interactions.[160] Quenchers are fluorophores that absorb electromagnetic radiation over a range of wavelengths but release heat instead of emitting light; they're commonly used as FRET acceptors.[161]

When developing a fluorescence biosensor, there's a vast pool of fluorophore options, however, physical and spectral properties such as photostability, size, solubility and compatibility with the desired bioconjugation are important to consider. Fluorophores can be separated into four categories: fluorescent proteins, organic dyes, quantum dots and metal chelates. Each type is accompanied by advantages and disadvantages that will influence the biosensors' performance; therefore, their suitability depends heavily on their application.[162]

Regarding fluorescence-based nanosensors, photoexcitation of the LFT strips is a widespread limiting factor. Carbon-based nanoparticles like fluorescent nanodiamonds (FNDs) are employed for biological applications because of their desirable properties, such as biocompatibility, physicochemical inertness, easy surface modification and magnetic field.[163] Le *et al.* developed a Spin-Enhanced Lateral Flow Immunoassay (SELFIA) for NS1 detection.[1] Their research demonstrated an enhancement in lateral flow test-line signals from incorporating a built-in fluorophore by utilising negatively charged nitrogen-vacancy (NV) centres in the fluorescent nanodiamond (FND) labels. The NV centres magnetically modulate the fluorescence intensity emitted when the FNDs are excited by a laser beam and subjected to a magnetic field.[1,164] Fluorescence emission is then collected by the objective lens, and a photomultiplier tube detects and transforms it into electrically modulated signals to be software-analysed. Thus, providing a background-free detection of FNDs on the lateral flow test line. Anti-NS1 antibodies were non-covalently conjugated to the carboxylated FNDS. These labels provide a 10-fold higher sensitivity when compared with conventional AuNPs. The sandwich SELFIA demonstrated an LOD of 0.1–1.3 ng mL^{-1} (DENV1 = 0.33 ng mL^{-1}, DENV2 = 0.24 ng mL^{-1}, DENV3 = 0.10, DENV4 = 1.33 ng mL^{-1}). This is beneficial for early dengue detection. Among the 4 serotypes, the binding affinity for DENV-4 was the lowest. Although the sandwich SELFIA provided a preferential LOD, direct SELFIA demonstrated the ability to distinguish between the serotypes and possessed an LOD of 0.5–2 μg mL^{-1}. Three different anti-NS1 antibodies were employed in this assay: Anti-NS1 mouse monoclonal antibody (Ms), anti-NS1 rabbit polyclonal antibody (Rb1) and anti-NS1 rabbit polyclonal antibody (Rb2). Serotyping was achieved by exploiting the binding affinities each antibody possessed for a specific DENV serotype.[1]

Chowdhury *et al.* presented a biosensing option for quantitative detection and serotyping of DENV infections,[94] by exploiting the metal-enhanced fluorescence (MEF) phenomenon.[165] MEF refers to the amplified fluorescence of a fluorophore in close proximity to metallic NPs or films.[165,166] Distance-dependent LSPR between AuNPs, and cadmium selenide tellurium sulphide fluorescent quantum dots (CdSeTeS QDs) underpins the basis for the sensor. The equilibrium between the local field enhancement effect and the non-radiative energy transfer (NRET) between the CdSeTeS QDs to the AuNPs is responsible for the quenching and enhancement of the fluorescence, see Fig. 9. Four ssDNA hairpin structures were designed for DENV detection, composed of a self-complementary conserved region formed from six cytosine (poly-(C)) and six guanine (poly-(G)) bases positioned on either side of the loop regions. Each loop sequence was complementary to the ssDNA/RNA from one of the DENV serotypes. The hairpin sequences for DENV-1 and DENV-3 were covalently bonded to CdSeTeS QDs at 5′poly-(C) end, whereas the sequences for DENV-2 and DENV-4 were bound at the 3′poly-(G) end. The AuNPs were functionalised with thiolated poly-(C). The CdSeTeS QDs and AuNPs only interact when complementary DENV ssDNA/RNA is present because the hybridisation between the loop region and the target ssDNA/RNA causes the

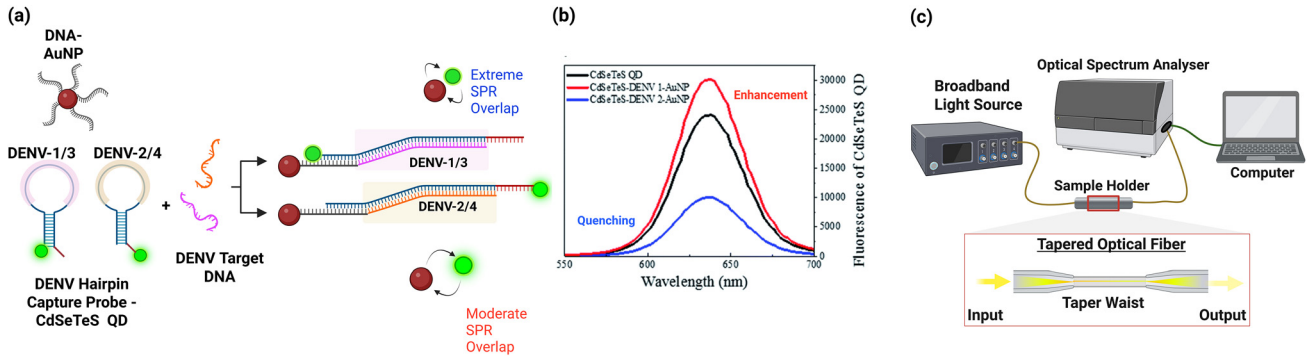

Fig. 9 (a) Diagram representing the detection of DENV1–4 ssDNA using hairpin ssDNA-CdSeTeS QDs and functionalised AuNPs, including the simplified structures of the DENV-1/3 and DENV-2/4 hairpin sequences, with the complementary loop regions for binding to the target DNA highlighted in pink (DENV-1/3) and cream (DENV-2/4), and a visual representation of the distance-based LSPR effect of AuNPs on CdSeTeS QDs, [reproduced and adapted].[94] (b) Fluorescence spectra of CdSeTeS QDs, and the nanocomposites CdSeTeS QDs–dsDNA–AuNP with DENV 1 and DENV 2 [reproduced, copyright © The Royal Society of Chemistry 2020].[94] (c) Schematic representation of the experimental setup used for TOF detection of DENV-2 E-proteins, including a simple illustration of a tapered optical fiber.[106,168] Created in BioRender. Etienne, R. (2025) https://BioRender.com/58ysdon.

hairpin structure to open, leaving the poly-(G) region free to bind to the poly-(C) AuNP. The distance between the AuNP and the CdSeTeS QD is determined by the serotype present. When DENV-1/3 ssDNA/RNA is bound, the CdSeTeS QDs are distanced ~14 nm away from the AuNPs. This triggers an enhancement of the QD's fluorescence, resulting from a significant local field enhancement effect. When DENV-2/4 ssDNA/RNA is bound, fluorescence is quenched due to the shorter distance (~3 nm), resulting in an extremely close overlap of SPR and non-radiative energy transfer dominates over the local field enhancement effect. Differing fluorescent intensities were associated with each serotype, allowing for differentiation. The biosensor's LODs for synthetic ssDNAs of DENV-1, 2, 3 and 4 were 24.6, 11.4, 39.8 and 39.7 fM, respectively. Unfortunately, detecting DENV RNA in clinical samples was less successful due to different interactions between DNA/DNA and RNA/DNA. Therefore, a reverse-transcription step could be considered for improved results for clinical applications. Additionally, this was the first attempt at amplification-free dengue serotyping with quantification at the time.[94,167]

4.2.4 Optical fiber based. Optical fiber sensing has proved advantageous for dengue detection due to the following characteristics: portable devices, easy operation, cost-effectiveness and small sample volumes. Camara *et al.* developed a sensing platform based on the specular reflection of AuNPs, in addition to LSPR.[86] This optical fiber nanosensor could detect concentrations of NS1 as low as 0.074 μg mL^{-1} (1.54 nM), which is within the circulating concentration range. Thus, providing a diagnostic technique suitable for acute dengue infections; however, improving the LOD could broaden the detection window. The advantage of a lowered LOD is the ability to efficiently catch DENV infections early, especially before they're presented with the opportunity to evolve into severe dengue. The sensor was composed of three parts: a white light source connected to a 2 × 1 optical fiber with a multimode fiber and a detector. The sample fiber was spliced into two; the sensing element was located on the free end (unspliced). The sensing element consisted of immobilised anti-NS1 antibodies on AuNPs on the tips of each fiber sample, with a set-up of (1) Optical fiber, (2) Gold NP Film, (3) Ligand for antibody binding, and (4) anti-NS1 antibody or glycine. Glycine acted as a protective measure to eliminate unwanted binding of analytes to the ligand's free amides, reducing possible false positives.[86] The time taken for sample immersion on the sensor for detection varied between 0.5–1 h, both time frames yielded similar results.

In contrast, Kamil *et al.* exploit the organic nanoparticle polyamidoamine (PAMAM) and Anti-dengue E-protein antibodies for the detection of the DENV-2 E-protein.[106] Their biofunctionalized tapered optical fiber-based sensor (TOF) was sensitive to any changes in the external medium, allowing the detection of an E-protein binding to the antibody. Unlike the more conventional optical fibers, a uniform cylindrical structured optical fibre is not included; instead, a tapered structure is present, see Fig. 9. The interaction between the evanescent waves and the external medium was measured using the interferometric method. Changes to the effective refractive indices of the broadband light propagating through the fiber were measured using an optical spectrum analyser to determine wavelength shifts.[106,168] Whereby, DENV-2 E-protein detection relies on the consistent power-independent wavelength-based output from the sensor.[106] The advantage of incorporating PAMAM is the resultant increase in the adhesion of the biorecognition molecules, Anti-Dengue E-protein antibodies. The PAMAM has an abundance of terminal amino and carboxyl functional groups on its dendritic branches. Creating an optimal binding environment for the antibodies to be absorbed. PAMAM not only provided a larger surface area for antibody binding but also resulted in more efficient tail-on position-bound antibodies. In turn, increasing both the number of anti-E protein antibodies in the preferred orien-

tation and E-protein immobilisation potential, as it's directly related to binding site availability. DENV-2 E-protein's presence was determined by a 0.72 nm red shift incurred, compared to the indistinguishable wavelength shift with target absence or Avidin (negative control). The biosensor presented a low LOD of 1 pM, creating a highly competitive alternative to recently developed diagnostics.[106]

Jeningsih *et al.* curated a sandwich-type DNA microoptode,[95] based on optical reflectance determination of DENV-2 DNA in samples using DNA recognition and capture probes. The optical label is a submicrometric-sized AuNP-labelled polyelectrolyte-coated poly(styrene-*co*-acrylic acid) (PSA) latex particle. The AuNPs coating the latex particles were ~20 nm (±5 nm) in diameter. Poly(*n*-butyl acrylate) (poly(*n*BA-NAS)) microspheres formed the DNA hybridisation platform for the sensor. The capture component consisted of aminated DNA capture probes (pDNA) covalently bound to the poly(*n*BS-NAS) microspheres *via* peptide bonds. The reporter DNA probe (rDNA) was immobilised on the gold-latex particles by thiol bonds, thus forming the detection component of the sandwich assay. Both rDNA and pDNA's sequences are complementary to sections of DENV-2's DNA. The target DNA (DENV-2) undergoes pre-hybridisation with the AuNP-PSA-rDNA, and these complexes are then introduced to the immobilised pDNA. The recognition and binding interaction between the target DNA to the pDNA elicits a violet-hued solution in the acrylic microsphere pDNA supporting matrix, visible to the naked eye. The fiber-optical reflectance spectrophotometer then detects colour changes and quantifies the DENV-2 DNA concentration. Thus, presenting a dual application for this assay: (1) A portable colourimetric DENV-2 diagnostic sensor for naked eye confirmation. (2) A sensitive fiber-optic colourimetric sensor for DENV-2 detection and quantification in reduced resource settings. The LOD for the device was 1.00×10^{-21} M for the concentration of DENV-2 DNA, with a hybridisation time of 90 min. This application required a reverse transcription step to form target DNA from DENV-2 RNA; eliminating this would drastically improve this sensor's efficiency for dengue detection. Producing a nanosensor more suited for POC/at-home DENV testing.[95]

4.2.5 Anisotropic nanoparticle-based optical biosensors. The previous sections have been divided by the operating principles the optical nanosensors were based on; however, this section will highlight the role anisotropic NPs have played in optical nanosensor advances for DENV. Variations of NPs can play the role of both labelling elements and transducers.[75] A AuNP's optical and electronic properties depend upon its shape and size. This forms the basis of many LSPR phenomena studies, but also, these NPs characteristically have optimal surface-binding abilities.[169–171] AuNPs possessing strong light scattering and absorption are demonstrated to be particularly advantageous in diagnostics. Equal volumes of gold nanorods (AuNRs) compared to spheres (AuNSPhs) demonstrate optical absorption efficiencies at least 20 times greater.[172] To further display the influence of a nanoparticle's shape, the scattering coefficients of AuNRs have been documented to be an order of magnitude higher than AuNSPhs and Au nanoshells.[173] Higher aspect ratio AuNRs possessing smaller effective radii are considered to be better photo-absorbent NPs, in contrast to high aspect ratio AuNRs with larger effective radii, which provide the highest scattering.[170]

The LSPR peak of gold nanostars (AuNSs) is highly tuneable; therefore, it may be located throughout the visible region and into the NIR region. The stars' structures, spikes, size and other characteristics, when altered, provide a method for creating an optimal SRP spectrum and optical profile. The varying, distinct colours associated with AuNS solutions are a result of the differing extinction profiles.[174,175] Induced aggregation of AuNSs presents colour changes for naked-eye detection in diagnostics. Tuning AuNSs LSPR peaks *via* blue or red-shifting provides a pathway for accessing the most dramatic aggregation-based colour changes, thus facilitating enhanced naked-eye detection.[175]

Furthermore, AuNFs are known to exhibit high optical brightness and improved sensitivity over conventional AuNSPhs, stemming from their multi-branched structures, resulting in high surface area to volume ratios.[176] In turn, this increases the binding avidity these NPs have for their target. Furthermore, NFs possess high LSPR absorption, owing to the interactions between the core and tips, providing an enhanced electromagnetic field. The large surface-to-volume ratio also affords high antibody loading capacity, much like AuNSs.[176]

4.2.5.1 Nanostar-based optical nanosensors.

Colourimetric: AuNS characteristics can be exploited when attempting to develop a more sensitive LFT. An alternative to the previously discussed DENV diagnostics indicates the surprising advantage of exploiting the cross-reactivity-induced false positives between the flavivirus family in diagnostic testing. The colourimetric biosensor possesses selective sensing resulting from using ELISA-screened DENV and ZIKV cross-reactive capture and detection antibodies.[177] Rodriguez-Quijada *et al.* exploited the difference in colours between AuNSPhs and AuNSs to label ZIKA and DENV-related antibodies. The antibody/antigen (Ab/Ag) interactions give rise to the possible differentiation between the three viral NS1 antigens, DENV, ZIKA and YFV. In the multiplexed NP shape LFT, AuNSs conjugated to anti-ZIKV polyclonal antibodies afford a blue spot, and AuNSPhs conjugated to anti-DENV-2 polyclonal antibodies produce a red spot. The red, green blue (RGB) colour differences between the blue AuNSs and the red spherical AuNPs and their appearance on the NC membrane allowed the viral antigens to be distinguished.[157,177] The lowest detection limit for the concentration of DENV NS1 antigens was 1.8 ng mL^{-1} when anti-DENV Abs were immobilised in the test area. This assay demonstrated the added ability of differentiating between DENV-1–4 with 92% accuracy, using pseudo colours and colour deconvolution. Colour deconvolution was required as the AuNS and AuNSPhs have an RGB overlap. Each serotype resulted in a red spot on the test strip, however, the colours varied slightly. Machine learning deciphered between the positive signal colours on the test strips by determining the contribution of each NP present for each serotype.[177]

Surface enhanced ramen spectroscopy: Raman scattering forms the basis for surface-enhanced Raman spectroscopy (SERS). It is an inelastic form of scattering, whereby the frequency of the incident photons can increase or decrease. This occurs due to the gain or loss of energy to the rotational and vibrational motions of the target analyte.[178,179] Whereas in elastic light scattering, the wavelength of the incident and scattered radiation (photons) remains unchanged (Rayleigh scattering),[178,179] see Fig. 10.[180] Raman spectra provide "fingerprints" for analyte identification as they include bands that correspond to vibrational/rotational transitions specific to a molecular structure.[179] SERS is an enhanced variation of standard Raman spectroscopy; the Raman signal intensity is increased by two mechanisms: a chemical mechanism and an electromagnetic mechanism.[179,181] The metallic structures used in SERS measurements need to be nanostructured, as electromagnetic enhancement depends on the collective oscillation of the electrons in noble metal NPs, roughened metal surfaces and sharp metal tips, as the LSPR excitation enhances the incident electric field intensity. Thus, electromagnetic enhancement is wavelength-dependent, and this is further confirmed by the observed maximum SERS intensity arising when the wavelength of the excitation laser is tuned to the LSPR maximum of the substrate used.[178,179] Nanospheres, nanoshells, nanoholes, and spiked/branched nanoparticles possess tunable optical properties, making them desirable for SERS-based sensing. Raman signal enhancement from the chemical mechanism is attributed to the chemisorption of a molecule to the metal's surface, which allows the surface electrons to interact with the molecule.[179] There are two main SERS configurations utilised in biosensing, intrinsic (direct and indirect) and extrinsic detection, see Fig. 10.[181,182] An analyte directly interacts with the bioreceptors immobilised on the nanostructured surface, and the spectral differences between the before and after analyte capture can be used for intrinsic detection. However, a Raman reporter generates the signal in extrinsic detection; thus, Raman reporters are immobilized on a nanostructure so the functionalized NP could be used for detection, Fig. 10.[181]

SERS-based biosensors for dengue detection utilising anisotropic metallic nanoparticles are examples of extrinsic detection, and the most common application associated with gold nanostars in dengue biosensing is for the enhancement of SERS.[183–185] The advantage of multiplexing within dengue diagnostics is demonstrated further by a multiplexed dipstick sandwich assay that utilises the high sensitivity present in SERS to result in more sensitive Dengue and Zika detection.[185] Like the majority of dengue diagnostics, NS1 is the target analyte for both viruses. SERS-encoded AuNS form the basis of this assay. Whereby the Ab-NP conjugates were AuNS-1,2-bis(4-pyridyl) ethylene (BPE) conjugated to anti-zika Abs (Z-nanotags) or AuNS-4-mercaptobenzoic acid (MBA) attached to anti-dengue Abs (D-nanotags). Thus, allowing the differentiation between infections, as the MBA and BPE molecules absorbed onto the surfaces of the nanostars acted as Raman reporters. Human serum samples indicated the LOD for the

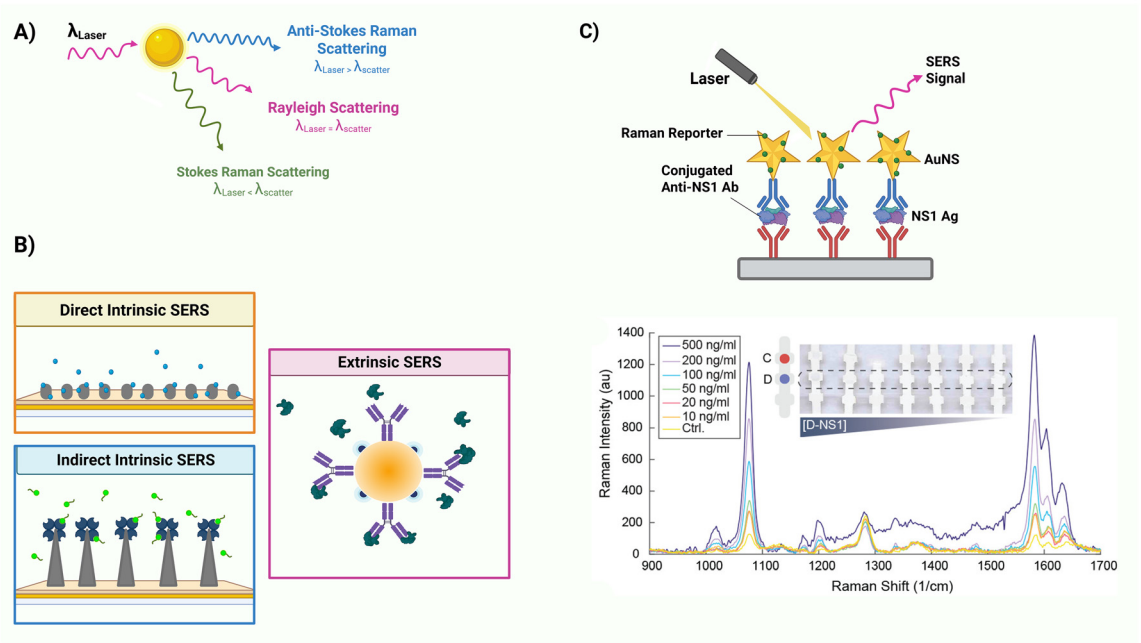

Fig. 10 (A) Visual representation of the three types of scattering that occur when a molecule is subjected to an intense laser of monochromatic light (visible/near-infrared/near-ultraviolet).[180] (B) Schematic representation of the strategies used for SERS detection classified as direct/indirect intrinsic and extrinsic detection (Raman reporters are immobilised onto the nanoparticle's surface).[181,182] (C) Visual example of a LFT sandwich assay formed by a capture anti-NS1 antibody, NS1 and a gold nanostar-antibody conjugate. In addition to the SERS spectra of LFT test-line where decreasing concentrations of DENV NS1 were used (500 to 10 ng mL^{-1}. Control = 0 ng mL^{-1} NS1).[183] Created in BioRender. Etienne, R. (2025) https://BioRender.com/ggtg1vr.

DENV naked eye visual readout was 55.3 ng mL^{-1}, compared to the seven-fold improvement for the SERS-related LOD of 7.67 ng mL^{-1}. For commercial dengue diagnostics, the reported LOD for the SD BIOLINE Dengue NS1 LFT is 37 ng mL^{-1}. Thus, indicating some space for visual colourimetric assay improvement to rival the commercially available LFTs.[185]

4.2.5.2 Nano rod-based optical sensors.

LSPR-based detection: Conjugation of bioreceptors to AuNRs is considerably efficient due to the strong binding affinity exhibited by AuNRs to thiol groups.[173] The aspect of cross-reactivity within the Flavivirus family is continuously highlighted, and there's a growing importance of differentiating between Flavivirus infections in testing. ZIKV emergence alongside high DENV seroprevalence has led to the increased possibility of false positives. AuNRs functionalized with *E. coli*-derived serospecific DENV-1–4 recombinant E-proteins can be enlisted for DENV-positive and ZIKV-positive sera analysis, *via* an in-house ELISA for human IgG detection. Presenting a sensitivity of 50.9 to 80.2% for DENV and ZIKA differentiation, respectively.[186] CTAB (cetyltrimethylammonium bromide) stabilised AuNRs are functionalised by ester bridge formation between the E-proteins and the dihydro-α-lipoic acid (DHLA) on the NP surfaces. DHLA is the capping agent responsible for reacting with sulfo-NHS (*N*-hydroxysulfosuccinimide) and EDC (1-ethyl-3-(3-dimethylaminopropyl)carbodiimide) to form a covalent bond. Assay efficiency and LOD measurements were investigated using diluted samples from a panel of antibodies/human patient sera and commercial monoclonal anti-Dengue antibodies, respectively. UV-Vis shift analysis resulting from the immobilisation of human anti-DENV-1–4 antibodies on the AuNR surface indicated an LOD of 1 pg when compared to the negative sera control. Versiani *et al.* also demonstrated serospecific nanosensors, with the ability to distinguish between infecting DENV serotypes. UV–Vis spectroscopy determined that the AuNR-DENV-4 E-protein sensor exhibited no DENV serotype-related or ZIKV-related cross-reactivity. DENV-1–3 E-protein sensors demonstrated a slightly reduced performance. Despite this, the sensitivity and specificity, encompassing all DENV serospecific sensors, remained high with 75% to 100% sensitivity and 88.2–100% specificity.[186] Alternatively, the use of eukaryote-derived (mouse, rabbit, human, *etc.*) recombinant proteins provides an avenue for possible improvements to the sensor's sensitivity and/or specificity.[187]

Colourimetric-based detection: Thanh *et al.* produced a colourimetric thermal sensing LFT with the ability to reduce the LOD associated with recombinant DENV-2 NS1 antigen detection by 4 times when compared to a conventional DENV-2 NS1 colourimetric LFT.[188] The thermal sensing assay format consisted of a thermochromic sheet, therefore, the increase in temperature resulted in visible colour changes. The LFT format investigated four different plasmonic NPs, AuNSPhs (12 nm) and AuNRs (LSPR 560 nm, 600 nm, 625 nm), alongside two MNPs; iron oxide (IONPs) and zinc ferrite (ZFNPs), to uncover the best combination for enhanced photothermal properties. ZFNPs produced the highest temperature increase (24.9 °C), but a reduced number of 12 nm AuNPs produced a sufficient rise in temperature (16.9 °C), therefore, they were selected as the LFT's label. The conventional LFT format presented an LOD of 6.25 ng mL^{-1} for the recombinant DENV-2 NS1. In contrast, the thermal sensing LFT offered an LOD of 1.56 ng mL^{-1} for a detectable visual signal. This semi-quantitative format positively enhanced detection sensitivity in the absence of an infrared (IR) camera or any complicated technology. Potentially expanding thermal LFT applications for use in POC early diagnostics.[188]

Fluorescence-based detection: Nanorod-based sensors encompass more than AuNRs, zinc oxide nanorods (ZnO NRs) exhibit unique electrical and optical properties, as a member of the II–VI group of semiconductors.[189] ZnO NRs are considered to hold a piezoelectric property, as well as ferromagnetic properties, consequently providing the potential for spintronic devices. Photoluminescence and cathodoluminescence have been utilised for the investigation of ZnO nanostructures.[190] The advantage of these biocompatible NPs lies in their high immobilisation capacity and detection sensitivity, which in turn stems from the vast binding sites available for biomolecules.[191–193] ZnO NRs possess high surface areas, providing a desirable NP for nanosensor development.[190] Dengue diagnostic microfluidic devices with the inclusion of ZnO NRs demonstrate enhanced detection capabilities.[191,194] A DENV-3 microfluidic detection device was formulated using an immunofluorescent assay rooted in the interaction between DENV-3 viral particles and monoclonal anti-DENV-3 E-protein antibodies. Hydrothermally grown ZnO NRs, covalently functionalised by a silanization agent, (3-glycidyloxypropyl)trimethoxysilane (GPTMS), were immobilised on the surface of a glass slide to be encapsulated in the microfluidic channels. Monoclonal human anti-DENV-3 E-protein antibodies conjugated to the ZnO NRs *via* GPTMS form the capture antibodies for the DENV-3 viral particles. Monoclonal mouse anti-DENV-3 E-protein antibodies then bind to the target analyte within the chip, where the final Alexa Fluor® 488 (Abcam, Inc., Cambridge, UK) tagged goat anti-mouse IgG can undergo affinity binding, resulting in detectable fluorescence. The photolithography-fabricated microchip, with 4% GPTMS modified ZnO NRs exhibited a viral concentration LOD of 3.1×10^{-4} ng mL^{-1} (in buffer) for a detectable fluorescent signal. Although the focal point of this microfluidic is for viral particles, the impressively low LOD could be a developing pillar for the detection of alternative DENV biomarkers.[191]

4.3 Comparison of optical nanosensors

To better evaluate the performance of optical nanosensors covered in this review, we have systematically presented their target analyte, detection principle, NPs used, and the assay's performance (LOD, sensitivities and specificities, run-time, if applicable) in Table 6. A limited number of the nanosensors are POC or applicable for home settings, while the others are in the same vein as PCR and ELISA, which require sophisticated equipment and highly skilled staff. Furthermore, real clinical samples were not acquired or tested for all of the

Table 6 Reviewed biosensors for the detection of DENV, organised by target analyte, including their detection principle, nanoparticles used, the biosensors LOD, the sensitivity/specificity if applicable and the assay time

No.	Target	Detection principle	Nanoparticle use	LOD	Sensitivity|selectivity	Assay time	Ref.
1	NS1	EIS	N/A	0.05 ng mL^{-1} (PBS + BSA (0.1%) buffer solution), 0.02 ng mL^{-1} (undiluted serum)	N/A|N/A	~40 min	123
2	NS1	ECS	N/A	30.9 fg mL^{-1} (PBS), 41.8 fg mL^{-1} (undiluted serum)	N/A|N/A	~30 min	125
3	NS1	ELASA	N/A	12.5 nM (TDENV-3), 25 nM (TDENV-6a)	N/A|N/A	15 min–60 min	126
4	NS1	ELISA	N/A	DEN1-NS1 = 6.97 ng ml^{-1}; DEN2-NS1 = 6.91 ng ml^{-1}; DEN3-NS1 = 11.06 ng ml^{-1}; DEN4-NS1 = 4.10 ng ml^{-1}	N/A|N/A	~90 min	132
5	NS1	Colourimetric	Carbon black nanoparticles, gold nanoparticles (AuNPs)	57 ng mL^{-1} (carbon black nanoparticles), 575 ng mL^{-1} (AuNPs)	N/A|N/A		158
6	NS1	Colourimetric	Gold nanoparticles	31.25 ng mL^{-1} (DENV-1, DENV-2, DENV-4), 15.625 ng mL^{-1} (DENV-3)	DENV-1 90%|98.74%; DENV-288.24%|96.13%; DENV-3 82.61%|99.39%; DENV-4 83.33% |97.04%	15 min	68
7	NS1	Fluorescence	Fluorescent nanodiamond (FND)	DENV-1 = 0.33 ng mL^{-1}; DENV-2 = 0.24 ng mL^{-1}; DENV-3 = 0.10 ng mL^{-1}; DENV-4 = 1.33 ng/mL	N/A|N/A	32 min–60 min	1
8	NS1	Optical fiber	Gold nanoparticle film	0.074 μg mL^{-1} (1.54 nM)	N/A|N/A	30 min–60 min	86
9	NS1	SPR	Silver nanoparticles (AgNPs)	~0.06 μg mL^{-1}	N/A|N/A	30 min	153
10	NS1	Colourimetric	Magnetic nanoparticles (MNPs)	N/A	91.9%|98.4%	12 min	154
11	NS1	ELISA	Gold nanostars (AuNSs)	1.8 ng mL^{-1}	N/A|92%	N/A	177
12	NS1	Thermal	Gold nanoparticles	1.56 ng mL^{-1}	N/A|N/A	N/A	188
13	NS1	SERS	Gold nanostars and Gold nanospheres	55.3 ng mL^{-1} (visual); 7.67 ng mL^{-1} (SERS)	N/A|N/A	N/A	185
14	ED3	Colourimetric	Gold nanoparticles and Iron oxide nanoparticles	Mixed DENV-1–4 pool = 10^6 $TCID_{50}$	N/A|N/A	N/A	127 and 196
15	ED3	Fluorescence	DNA nanostructures	Human serum = 1 × 102 pfu mL^{-1}, Plasma = 1 × 103 pfu mL^{-1}	N/A|N/A	N/A	129
16	E-protein	Optical fiber	Polyamidoamine (PAMAM)	1 pM	N/A|N/A	15 min	106
17	E-protein	CLEIA	N/A	N/A	85.0%|96.4%	90 min	197
18	E-protein	Fluorescence	Zinc oxide nanorods (ZnO NRs)	3.1×10^{-4} ng mL^{-1}	N/A	N/A	191
19	DNA	Fluorescence	Silver nanocluster	N/A	N/A|N/A	N/A	137
20	DNA	Optical fiber	Gold nanoparticles	1.00×10^{-21} M	N/A|N/A	90 min	95
21	RNA	Colourimetric	Plasmonic magnetic nanoparticles (PMNs)	1.6 copies per μL	N/A|N/A	N/A	159
22	RNA	Colourimetric	Gold nanoparticles	~250 pg μL^{-1} (~4.15×10^8 RNA copies)	N/A|N/A	N/A	38
23	RNA	Colourimetric	Dextrin-capped gold nanoparticles	1.2×10^4 pfu mL^{-1}	N/A|N/A	N/A	104
24	RNA/ssDNA	Fluorescence	Gold nanoparticles and cadmium selenide tellurium sulphide fluorescent quantum dots (CdSeTeS QDs)	DENV-1 = 24.6 fM; DENV-2 = 11.4 fM; DENV-3 = 39.8 fM; DENV-4 = 39.7 fM	N/A|N/A	N/A	94 and 167
25	IgG	LSPR	Gold nanorods (AuNRs)	1 pg	75–100%|88.2–100%	N/A	186
26	IgG	ELISA	N/A	1.19–2.36 ng ml^{-1} (buffer); 1.14–3.31 ng ml^{-1} (serum)	N/A|N/A	~120 min	132

sensors, thus hindering their assessments for real-life performance. These sensors (in Table 6) and conventional DENV diagnostics predominantly employ antibodies or RNA sequences as bioreceptors, while enzyme, aptamer (targeting DENV antigens), cell receptor, and whole-cell-based detection is still lacking. Integration of diverse biorecognition elements indicates a promising path for enhancing DENV tests. The commercial LFTs utilise AuNPs; however, further sensitivity

Table 7 Comparative table of the key advantages and disadvantages of the commercial test and optical nanosensors

Target analyte		Commercial detection	Nanosensor detection
Genetic material	Method		
	PCR	**Advantages** • Gold standard • Desirable sensitivity and selectivity data • Same/next day results • Serotyping available • Whole blood, serum, plasma, and cerebrospinal fluid applicable **Disadvantages** • Highly costly • Highly intensive • Requires special equipment • Minimal POC options • Sample pre-treatment (RNA extraction)	**Advantages** • Real-time detection • Short assay-run time • High sensitivity • Easy to operate • Inexpensive **Disadvantages** • Sample pretreatment (RNA extraction and ssDNA/dsDNA translation) • Requires sophisticated equipment • Unavailable sensitivity and specificity percentages • Small sample type variation
	PCR mimics (isothermal/loop mediated amplification)	**Advantages** • Minimal sample pre-treatment • Portable/compact devices • Desirable sensitivity and selectivity data • Minimised human error **Disadvantages** • Requires special equipment • Costly • No serotyping possibilities • Not readily available	
NS1 and IgM/IgG	ELISA	**Advantages** • High sensitivity and specificity • Long shelf life • POC applicable **Disadvantages** • Time-consuming • Costly • Skilled personnel required • Requires equipment • Not home-testing applicable • Potential false positives due to flavivirus cross-reactive antibodies (IgM/IgG) • Large sample volume • Sample pre-treatment may be required	**Advantages** • Rapid • Enhanced sensitivity • Reduced cost • Potentially label-free • Less invasive • Reduced sample volumes • Potential to serotype • Easy to operate **Disadvantages** • Not all are serum, plasma and whole blood applicable • Not all are POC applicable • Reduced clinical sample testing • Unavailable sensitivity and specificity percentages • May require specific equipment • Not many IgG and IgM biosensors
	LFT	**Advantages** • Rapid assay run time • Long shelf life • POC applicable • Serum, plasma and whole blood applicable • Non-invasive • No sample pre-treatment required • Inexpensive **Disadvantages** • Undesirable sensitivities (NS1) • Not home-testing applicable • Low sensitivity	
E-protein	N/A	No options available	**Advantages** • High sensitivity • Short assay-run times **Disadvantages** • Requires sophisticated equipment • Not all are serum, plasma and whole blood applicable • Costly sensor fabrication • Not all are POC applicable • Reduced clinical sample testing • Unavailable sensitivity and specificity percentages

enhancement could be achieved by employing advanced nanoprobes, such as alternative NP compositions and morphologies.[195] A proportion of the NS1 targeting nanosensors demonstrate this by possessing competitive LODs, notably, the FND-based sensor (7),[1] the AuNS-based ELISA (11),[177] and the SERS-based LFT using AuNS probes (13).[185] Yet, none can be considered an 'ideal' RDT. Investigating the thermal properties of IONPs, ZFNPs, and conventional AuNPs provided an interesting avenue for enhancing the LFT test-line sensitivity using a thermochromic sheet to enable visual detection without sophisticated equipment. With an LOD below 4.8 ng mL^{-1} for DENV-2 detection and a user-friendly format, this innovative design shows great potential. Therefore, broadening the detection to encompass all DENV serotypes would make this test a strong candidate for an 'ideal' RDT. Some sensors also display advances in serotyping capabilities,[1,68,94,177,187] the AuNP-based LFT (6),[68] possesses the potential to serotype infections, alongside competitive LODs when compared to commercial LFTs, indicating it could be an advantageous addition to the market. It's also important to note that DENV E-protein detection has not been present in commercial testing; however, it has been explored as a potential target analyte.[127,129,186,191,196,197]

4.3.1 Commercial testing and optical nanosensors. From Table 7, there are clear advantages to nanosensor-based detection over commercial testing, especially for NS1 detection. Many of the nanosensors have rapid assay-run times, reduced costs and simplified operations, all qualities that are highly desirable for dengue testing. Additionally, their increased sensitivities and the potential reduction in sample volumes provide some promising avenues to help level up the current commercial diagnostic pool. Despite this, the nanosensors display a reduced number of IgG-based biosensors and no IgM biosensors; therefore, using commercial tests for serological-based detection is still preferable. Furthermore, nucleic acid-based detection has seen some positive developments, but these nanosensors still require sophisticated equipment, and there is also little variation in the types of samples used. Therefore, optimisation of these nanosensors is still required before they can rival the gold standard, PRC.

5. Conclusions and future perspectives

Recently published review articles on dengue diagnostics have focused primarily on electrical and optical-based sensing, but their nanoparticle components have not been a focal point. In this review, we highlight the nanoparticles utilised for each optical nanosensor discussed. Moreover, the background knowledge provided regarding NS1 antigenemia and commercial RDT LODs for DENV NS1 is also not featured in these articles. Our review presents major challenges for dengue diagnostics, such as low circulating biomarker concentrations, geographical variation in DENV strains, testing sample type, differences in primary and post-primary infection biomarker profiles and the lack of general regulations for diagnosis. The current reliance on laboratory-based tests, *e.g.* PCR and ELISA, owing to their high sensitivities and reliability, is impractical for efficient DENV testing, and despite the advantages of commercial LFTs, their performance is hindered by their sensitivities. Although several optical nanosensors exist, user-friendly RDTs that can outperform the current LFTs on the market and meet the WHO's 'REASSURED' test criteria are limited. Optimisation of the nanosensor's components, including the nanoprobe and bioreceptors used, is vital for increasing the overall efficiency of DENV tests.

For lateral flow testing, future improvements may involve post-binding aggregation-based signal-enhancement and fine-tuning the strip design for more effective binding to enhance future testing sensitivities. These considerations are especially crucial for developing highly sensitive, low-cost RDTs with improved NS1 LODs to not only aid in POC and home-setting testing, but also broaden the detection window. Further research into the circulating concentrations of DENV E-proteins and their use for serotyping infections is critical for fully realising this antigen's potential as a diagnostic target. Numerous commercial tests and optical nanosensors detect NS1, so diversifying the antigenomic targets used in diagnosis to include DENV E-proteins could elevate the capabilities of DENV testing.

From the nanosensors discussed, it is clear that rapid assay-run times, high sensitivities and simplicity are required for breaking into the commercial market. Currently, there are many benefits to using commercial testing options; however, the gold standard tests are accompanied by restricted access due to high costs and the sophisticated equipment required. Although some biosensors have simplified assays, many still also require sophisticated equipment. To effectively overcome this, optical nanosensors need to utilise other avenues for enhanced sensitivity by incorporating low-cost detection tools or smartphone-based detection. For example, RDTs can incorporate an optical nanosensor that implements more sophisticated techniques and is designed as a POC microfluidic or an assay to be analysed by a mobile phone. Furthermore, a breakthrough into the commercial market requires the nanosensors to be easily operated as well as easily distributed. Therefore, they must be able to withstand temperature changes and have a suitable shelf life. For POC testing, if equipment is necessary, simple, cheap, handheld devices would be preferable. These tests could hold great potential for levelling up the current state of optical nanosensing and allowing for a breakthrough into the commercial market.

Author contributions

Rhai-Anne A. C. Etienne: conceptualisation (supporting); wrote the original draft. Nguyen T. K. Thanh: conceptualisation (lead), critical reviewing. Yasuhiro Takeuchi: reviewing, Xiaodi Su: conceptualisation (lead), reviewing.

Conflicts of interest

There are no conflicts to declare.

Data availability

No primary research results, software or code have been included, and no new data were generated or analysed as part of this review.

Acknowledgements

This study was funded by the Agency for Science, Technology and Research (A*STAR) RIE2025 Human Health and Potential (HHP) Industry Alignment Fund—Pre-Positioning (IAF-PP) grant (H25J6a0016). R. A. C. Etienne thanks UCL and the ARAP program of A*STAR (Singapore) for the scholarship opportunity. BioRender.com was used alongside Adobe Firefly to create the cover artwork for this article. The graphical abstract was created in BioRender. Etienne, R. (2025) https://BioRender.com/vzdrm1j.

References

1 T.-N. Le, W. W.-W. Hsiao, Y.-Y. Cheng, C.-C. Lee, T.-T. Huynh, D. M. Pham, M. Chen, M.-W. Jen, H.-C. Chang and W.-H. Chiang, *Anal. Chem.*, 2022, **94**(51), 17819–17826.
2 M. B. Khan, Z.-S. Yang, C.-Y. Lin, M.-C. Hsu, A. N. Urbina, W. Assavalapsakul, W.-H. Wang, Y.-H. Chen and S.-F. Wang, *J. Infect. Public Health*, 2023, **16**(10), 1625–1642.
3 S. A. Kularatne and C. Dalugama, *Clin. Med.*, 2022, **22**, 9–13.
4 Dengue worldwide overview, https://www.ecdc.europa.eu/en/dengue-monthly, (accessed March 2025).
5 J. P. Messina, O. J. Brady, N. Golding, M. U. G. Kraemer, G. R. W. Wint, S. E. Ray, D. M. Pigott, F. M. Shearer, K. Johnson, L. Earl, L. B. Marczak, S. Shirude, N. Davis Weaver, M. Gilbert, R. Velayudhan, P. Jones, T. Jaenisch, T. W. Scott, R. C. Reiner and S. I. Hay, *Nat. Microbiol.*, 2019, **4**(9), 1508–1515.
6 European Centre for Disease Prevention and Control, Twelve-month dengue virus disease case notification rate per 100 000 population, August 2024–July 2025, https://www.ecdc.europa.eu/en/publications-data/twelve-month-dengue-virus-disease-case-notification-rate-100-000-population-0, (accessed 27/08, 2025).
7 O. Parkash and R. H. Shueb, *Viruses*, 2015, **7**(10), 5410–5427.
8 D. A. Muller, A. C. I. Depelsenaire and P. R. Young, *J. Infect. Dis.*, 2017, **215**, S89–S95.
9 J. M. Wong, L. E. Adams, A. P. Durbin, J. L. Muñoz-Jordán, K. A. Poehling, L. M. Sánchez-González, H. R. Volkman and G. Paz-Bailey, *Pediatrics*, 2022, **149**(6), e2021055522.
10 P. B. Deroco, D. W. Junior and L. T. Kubota, *Sens. Actuators, B*, 2021, **349**, 130821.
11 S. S. Hegde and B. R. Bhat, *Biosens. Bioelectron.: X*, 2022, **10**, 100100.
12 R. Eivazzadeh-Keihan, P. Pashazadeh-Panahi, T. Mahmoudi, K. K. Chenab, B. Baradaran, M. Hashemzaei, F. Radinekiyan, A. Mokhtarzadeh and A. Maleki, *Mikrochim. Acta*, 2019, **186**(329).
13 J. V. L. Macêdo, A. G. S. Júnior, M. D. L. Oliveira and C. A. S. Andrade, *Diagn. Microbiol. Infect. Dis.*, 2024, **109**(2), 116227.
14 G. Paz-Bailey, L. E. Adams, J. Deen, K. B. Anderson and L. C. Katzelnick, *Lancet*, 2024, **403**(10427), 667–682.
15 G. N. Malavige, C. Jeewandara and G. S. Ogg, *J. Biomed. Sci.*, 2022, **29**, 48.
16 S. Sinha, K. Singh, Y. S. R. Kumar, R. Roy, S. Phadnis, V. Meena, S. Bhattacharyya and B. Verma, *J. Biomed. Sci.*, 2024, **31**(43).
17 G. Lebeau, A. Lagrave, E. Ogire, L. Grondin, S. Seriacaroupin, C. Moutoussamy, P. Mavingui, J.-J. Hoarau, M. Roche, P. Krejbich-Trotot, P. Desprès and W. Viranaicken, *Vaccines*, 2021, **9**(9), 946.
18 P. Bhatt, S. P. Sabeena, M. Varma and G. Arunkumar, *Curr. Microbiol.*, 2021, **78**, 17–32.
19 B. E. E. Martina, P. Koraka and A. D. M. E. Osterhaus, *Clin. Microbiol. Rev.*, 2009, **22**(4), 564–581.
20 A. Tayal, S. K. Kabra and R. Lodha, *Indian J. Pediatr.*, 2023, **90**, 168–177.
21 World Health Organization, UNICEF/UNDP/World Bank/WHO Special Programme for Research Training in Tropical Diseases Research, *Handbook for clinical management of dengue*, World Health Organization, Geneva, 2012.
22 M. R. Hasan, P. Sharma, S. Khan, U. M. Naikoo, K. Bhalla, M. Z. Abdin, N. Malhotra, T. M. Aminabhavi, N. P. Shetti and J. Narang, *Sens. diagn.*, 2025, **4**, 7–23.
23 Countries/territories reporting dengue cases since April 2023, and as of May 2024, https://www.ecdc.europa.eu/en/publications-data/countriesterritories-reporting-dengue-cases-april-2023-and-may-2024, (accessed 10/07/2024, 2024).
24 A. Teo, H. D. Tan, T. Loy, P. Y. Chia and C. L. L. Chua, *PLoS Pathog.*, 2023, **19**(3), e1011223.
25 K. Yuan, Y. Chen, M. Zhong, Y. Lin and L. Liu, *PLoS One*, 2022, **17**(4), e0267186.
26 S. B. Halstead, *Science*, 1988, **239**(4839), 476–481.
27 M. G. Guzman, D. J. Gubler, A. Izquierdo, E. Martinez and S. B. Halstead, *Nat. Rev. Dis. Primers*, 2016, **2**, 16055.
28 D. B. Shrestha, P. Budhathoki, B. Gurung, S. Subedi, S. Aryal, A. Basukala, B. Aryal, A. Adhikari, A. Poudel, G. K. Yadav, M. Khoury, B. Rayamajhee and L. B. Shrestha, *Parasites Vectors*, 2022, **15**, 389.
29 P. F. H. Bautista, D. A. C. Gaytán, C. E. S. Tinoco, A. V. Parás, J. E. A. Yaah, B. M. Miguel, Y. M. A. Hernández, L. A. Nieto, A. M. Paz, L. J. Betancourt, Y. P Andrade, O. C. Orozco, G. V. Alvarado and M. G. R. Mahey, *Viruses*, 2024, **16**(5), 769.

30 S. Kalayanarooj and S. Nimmannitya, *Clinical and laboratory presentations of dengue patients with different serotypes*. WHO Regional Office for South-East Asia, 2000, https://iris.who.int/handle/10665/148790.
31 P. Rao, A. Basavaprabhu, S. Shenoy, N. V. Dsouza, B. Sridevi Hanaganahalli and V. Kulkarni, *Int. J. Microbiol.*, 2020, **2020**, 6658445.
32 A. Gupta, P. Rijhwani, M. R. Pahadia, A. Kalia, S. Choudhary, D. P. Bansal, D. Gupta, P. Agarwal and R. K. Jat, *Cureus*, 2021, **13**, e15029.
33 R. Aguas, I. Dorigatti, L. Coudeville, C. Luxemburger and N. M. Ferguson, *Sci. Rep.*, 2019, **9**(9395).
34 S. Zannoli, M. Morotti, A. Denicolò, M. Tassinari, C. Chiesa, A. Pierro and V. Sambri, in *Chikungunya and Zika Viruses*, ed. S. Higgs, D. L. Vanlandingham and A. M. Powers, Academic Press, 2018, pp. 293–315. DOI: 10.1016/B978-0-12-811865-8.00009-X.
35 A. R. Plourde and E. M. Bloch, *Emerging Infect. Dis.*, 2016, **22**, 1185–1192.
36 E. S. Paixão, F. Barreto, M. G. Teixeira, M. C. Costa and L. C. Rodrigues, *Am. J. Public Health*, 2016, **106**(4), 606–612.
37 L. Kittigul, P. Pitakarnjanakul, D. Sujirarat and K. Siripanichgon, *J. Clin. Virol.*, 2007, **39**(2), 76–81.
38 V. T. C. Duyen, V. Van Toi, T. Van Hoi and P. L. Truong, *Anal. Methods*, 2023, **15**, 3991–3999.
39 Y. Xu, L.-Z. Zhao, Y.-Z. Xu, J.-B. Gu, K. Wu, Z.-Q. Peng, X.-H. Zhou, F.-C. Zhang and X.-G. Chen, *Infect. Dis. Poverty*, 2020, **9**(17).
40 CDC, Molecular Tests for Dengue Virus, https://www.cdc.gov/dengue/hcp/diagnosis-testing/molecular-tests-for-dengue-virus.html, (accessed October 2024).
41 World Health Organisation, *Dengue guidelines for diagnosis, treatment, prevention and control: new edition*, World Health Organization, Geneva, 2009. Report 9789241547871.
42 M. A. Kabir, H. Zilouchian, M. A. Younas and W. Asghar, *Biosensors*, 2021, **11**(7), 206.
43 J.-J. Tsai, W.-L. Liu, P.-C. Lin, B.-Y. Huang, C.-Y. Tsai, P.-H. Chou, F.-C. Lee, C.-F. Ping, P.-Y. A. Lee, L.-T. Liu and C.-H. Chen, *PLoS One*, 2019, **14**, e0214328.
44 J.-J. Tsai, W.-L. Liu, P.-C. Lin, B.-Y. Huang, C.-Y. Tsai, P.-Y. A. Lee, Y.-L. Tsai, P.-H. Chou, S. Chung, L. T. Liu and C.-H. Chen, *PLoS One*, 2019, **14**(7), e0218139.
45 S. Alcon-LePoder, M. Drouet, P. Roux, M. Frenkiel, M. Arborio, A. Durand-Schneider, M. Maurice, I. Le Blanc, J. Gruenberg and M. Flamand, *J. Virol.*, 2005, **79**, 11403–11411.
46 B. L. A. Chew, Q. Pan, H. Hu and D. Luo, *Antiviral Res.*, 2024, **227**, 105915.
47 A. C. Alcalá and J. E. Ludert, *PLoS Pathog.*, 2023, **19**(8), e1011587.
48 S. Alcon, A. Talarmin, M. Debruyne, A. Falconar, V. Deubel and M. Flamand, *J. Clin. Microbiol.*, 2002, **40**(2), 376–381.
49 D. Allonso, M. D. F. Meneses, C. A. Fernandes, D. F. Ferreira and R. Mohana-Borges, *PLoS One*, 2014, **9**(11), e113634.
50 M. Haider, S. Yousaf, A. Zaib, A. Sarfraz, Z. Sarfraz and I. Cherrez-Ojeda, *Int. J. Environ. Res. Public Health*, 2022, **19**(14), 8756.
51 S.-C. Lai, Y.-Y. Huang, P.-Y. Shu, S.-F. Chang, P.-S. Hsieh, J.-J. Wey, M.-H. Tsai, R.-J. Ben, Y.-M. Hsu, Y.-C. Fang, M.-L. Hsiao and C.-C. Lin, *J. Clin. Microbiol.*, 2019, **57**(7), e00221.
52 D. A. Martin, D. A. Muth, T. Brown, A. J. Johnson, N. Karabatsos and J. T. Roehrig, *J. Clin. Microbiol.*, 2000, **38**(5), 1823–1826.
53 CDC, Clinical Testing Guidance for Dengue, https://www.cdc.gov/dengue/healthcare-providers/diagnosis.html, (accessed 17/04, 2025).
54 H. Lee, J. H. Ryu, H.-S. Park, K. H. Park, H. Bae, S. Yun, A.-R. Choi, S.-Y. Cho, C. Park, D.-G. Lee, J. Lim, J. Lee, S. Lee, S. Shin, H. Park and E.-J. Oh, *Ann. Lab. Med.*, 2019, **39**(6), 566–571.
55 L. Osorio, M. Ramirez, A. Bonelo, L. A. Villar and B. Parra, *Virol. J.*, 2010, **7**(361).
56 S. Pal, A. L. Dauner, I. Mitra, B. M. Forshey, P. Garcia, A. C. Morrison, E. S. Halsey, T. J. Kochel and S.-J. L. Wu, *PLoS One*, 2014, **9**, e113411.
57 L. A. Sánchez-Vargas, E. E. Sánchez-Marce and H. Vivanco-Cid, *Diagn. Microbiol. Infect. Dis.*, 2014, **78**, 368–372.
58 N. Raafat, S. D. Blacksell and R. J. Maude, *Trans. RSTMH*, 2019, **113**, 653–660.
59 M. Rashiku, K. Manoharan, N. Rani, J. Samal, E. Gupta and S. Bhattacharya, *J. Clin. Virol. Plus*, 2023, **3**(2), 100144.
60 C. Gaspar-Castillo, M. H. Rodríguez, V. Ortiz-Navarrete, C. M. Alpuche-Aranda and J. Martinez-Barnetche, *Front. Microbiol.*, 2023, **14**, 1107496.
61 W. A. A. Saron, A. P. S. Rathore, L. Ting, E. E. Ooi, J. Low, S. N. Abraham and A. L. St John, *Sci. Adv.*, 2018, **4**(7), eaar4297.
62 A.-C. Andries, V. Duong, C. Ngan, S. Ong, R. Huy, K. K. Sroin, V. Te, P. Lorn Try and P. Buchy, *PLoS Neglected Trop. Dis.*, 2012, **6**, e1993.
63 WHO Republic of Timor-Leste Department of Communicable Diseases, Ministry of Health Democratic Republic of Timor-Leste, *National Guideline for Clinical Management of Dengue 2022*, Timor-Leste, 2022.
64 T. H. T. Nguyen, H. E. Clapham, K. L. Phung, T. K. Nguyen, T. T. DInh, T. H. Q. Nguyen, V. N. Tran, S. Whitehead, C. Simmons, M. Wolbers and B. Wills, *BMC Infect. Dis.*, 2018, **18**(1), 375.
65 R. W. Peeling, H. Artsob, J. L. Pelegrino, P. Buchy, M. J. Cardosa, S. Devi, D. A. Enria, J. Farrar, D. J. Gubler, M. G. Guzman, S. B. Halstead, E. Hunsperger, S. Kliks, H. S. Margolis, C. M. Nathanson, V. C. Nguyen, N. Rizzo, S. Vázquez and S. Yoksan, *Nat. Rev. Microbiol.*, 2010, **8**, S30–S37.
66 M. Haider, S. Yousaf, A. Zaib, A. Sarfraz, Z. Sarfraz and I. Cherrez-Ojeda, *Int. J. Environ. Res. Public Health*, 2022, **19**(14), 8756.
67 K. Suzuki, E. E. Nakayama, A. Saito, A. Egawa, T. Sato, J. Phadungsombat, R. Rahim, A. Hasan, H. Iwamoto, M. Rahman and T. Shioda, *Virol. J.*, 2019, **16**(102).

68 S.-C. Lai, Y.-Y. Huang, J.-J. Wey, M.-H. Tsai, Y.-L. Chen, P.-Y. Shu, S.-F. Chang, Y.-J. Hung, J.-N. Hou and C.-C. Lin, *Front. Immunol.*, 2022, **13**, 852452.
69 S. R. Fry, M. Meyer, M. G. Semple, C. P. Simmons, S. D. Sekaran, J. X. Huang, C. McElnea, C.-Y. Huang, A. Valks, P. R. Young and M. A. Cooper, *PLoS Neglected Trop. Dis.*, 2011, **5**(6), e1199.
70 P. Pan, G. Li, M. Shen, Z. Yu, W. Ge, Z. Lao, Y. Fan, K. Chen, Z. Ding, W. Wang, P. Wan, M. A. Shereen, Z. Luo, X. Chen, Q. Zhang, L. Lin and J. Wu, *PLoS Pathog.*, 2021, **17**(7), e1008603.
71 A. T. Waickman, J. Q. Lu, H. Fang, M. J. Waldran, C. Gebo, J. R. Currier, L. Ware, L. Van Wesenbeeck, N. Verpoorten, O. Lenz, L. Tambuyzer, G. Herrera-Taracena, M. Van Loock, T. P. Endy and S. J. Thomas, *Sci. Transl. Med.*, 2022, **14**(668), eabo5019.
72 P. R. Young, P. A. Hilditch, C. Bletchly and W. Halloran, *J. Clin. Microbiol.*, 2000, **38**, 1053–1057.
73 P. C. G. Nunes, R. M. R. Nogueira, M. Heringer, T. Chouin-Carneiro, C. D. D. S Rodrigues, A. M. B. de Filippis, M. Lima and F. B. Dos Santos, *Viruses*, 2018, **10**(6), 326.
74 C.-H. Huang, L.-L. Kuo, K. D. Yang, P.-S. Lin, P.-L. Lu, C.-C. Lin, K. Chang, T.-C. Chen, W.-R. Lin, C.-Y. Lin, Y.-H. Chen and H.-S. Wu, *J. Microbiol., Immunol. Infect.*, 2013, **46**(5), 358–365.
75 V. Naresh and N. Lee, *Sensors*, 2021, **21**(4), 1109.
76 C. Chen and J. Wang, *Analyst*, 2020, **145**(5), 1605–1628.
77 K. J. Land, D. I. Boeras, X.-S. Chen, A. R. Ramsay and R. W. Peeling, *Nat. Microbiol.*, 2019, **4**, 46–54.
78 World Health Organisation, *Dengue: Guidelines for Diagnosis, Treatment, Prevention and Control: New Edition*, World Health Organization, Copyright © 2009, Geneva, 2009.
79 World Health Organization, Regional Office for South-East, *Comprehensive Guideline for Prevention and Control of Dengue and Dengue Haemorrhagic Fever, Revised and expanded edn*, WHO Regional Office for South-East Asia, New Delhi, 2011.
80 P. D. Mendonça, L. K. B. Santos, M. V. Foguel, M. A. B. Rodrigues, M. T. Cordeiro, L. M. Gonçalves, E. T. A. Marques and R. F. Dutra, *Anal. Bioanal. Chem.*, 2021, **413**(9), 4873–4885.
81 Q. Palomar, X. Xu, C. Gondran, M. Holzinger, S. Cosnier and Z. Zhang, *Mikrochim. Acta*, 2020, **187**, 363.
82 M. H. Nawaz, A. Hayat, G. Catanante, U. Latif and J. L. Marty, *Anal. Chim. Acta*, 2018, **1026**, 1–7.
83 J. Cecchetto, F. C. B. Fernandes, R. Lopes and P. R. Bueno, *Biosens. Bioelectron.*, 2017, **87**, 949–956.
84 R. Dutta, K. Thangapandi, S. Mondal, A. Nanda, S. Bose, S. Sanyal and S. Jana, *Avicenna J. Med. Biotechnol.*, 2020, **12**, 77–84.
85 W. R. Wong, S. D. Sekaran, F. R. M. Adikan and P. Berini, *Biosens. Bioelectron.*, 2016, **78**, 132–139.
86 A. R. Camara, P. M. P. Gouvêa, A. C. M. S. Dias, A. M. B. Braga, R. F. Dutra, R. E. de Araujo and I. C. S. Carvalho, *Opt. Express*, 2013, **21**(22), 27023–27031.
87 F. S. R. R. Teles, *Anal. Chim. Acta*, 2011, **687**(1), 28–42.
88 T. V. Tran, B. V. Nguyen, T. T. P. Nguyen, T. T. Tran, K. G. Pham, Q. B. Le, B. N. Do, H. N. Pham, C. V. Nguyen, D. P. H. Dinh, V. T. Ha, T. H. T. Doan and H. Q. Le, *PeerJ*, 2019, **7**, e7779.
89 N. T. Darwish, S. D. Sekaran, Y. Alias and S. M. Khor, *J. Pharm. Biomed. Anal.*, 2018, **149**, 591–602.
90 A. Santos, P. R. Bueno and J. J. Davis, *Biosens. Bioelectron.*, 2018, **100**, 519–525.
91 S. Solanki, A. Soni, M. K. Pandey, A. Biradar and G. Sumana, *ACS Appl. Mater. Interfaces*, 2018, **10**(3), 3020–3028.
92 J. H. Kim, C. H. Cho, M. Y. Ryu, J.-G. Kim, S.-J. Lee, T. J. Park and J. P. Park, *PLoS One*, 2019, **14**(9), e0222144.
93 Q. Y. Siew, E. L. Pang, H.-S. Loh and M. T. T. Tan, *Biosens. Bioelectron.*, 2021, **176**, 112895.
94 A. D. Chowdhury, K. Takemura, I. M. Khorish, F. Nasrin, M. M. N. Tun, K. Morita and E. Y. Park, *Nanoscale Adv.*, 2020, **2**, 699–709.
95 Jeningsih, L. L. Tan, A. Ulianas, L. Y. Heng, N.-F. Mazlan, N. D. Jamaluddin, N. Y. M. Yusof, B. Khalid and G. C. Ta, *Sensors*, 2020, **20**(7), 1820.
96 C. Song, J. Zhang, Y. Liu, X. Guo, Y. Guo, X. Jiang and L. Wang, *Sens. Actuators, B*, 2020, **325**, 128970.
97 A. D. Chowdhury, A. B. Ganganboina, F. Nasrin, K. Takemura, R.-a. Doong, D. I. S. Utomo, J. Lee, I. M. Khoris and E. Y. Park, *Anal. Chem.*, 2018, **90**, 12464–12474.
98 E. Y. Ariffin, L. L. Tan, N. H. A. Karim and L. Yook Heng, *Sensors*, 2018, **18**(4), 1173.
99 N.-F. Mazlan, L. L. Tan, N. H. A. Karim, L. Y. Heng and M. I. H. Reza, *Sens. Actuators, B*, 2017, **242**, 176–188.
100 M. M. Nuzaihan, U. Hashim, M. K. M. Arshad, S. R. Kasjoo, S. F. A. Rahman, A. R. Ruslinda, M. F. M. Fathil, R. Adzhri and M. M. Shahimin, *Biosens. Bioelectron.*, 2016, **83**, 106–114.
101 J. I. A. Rashid, N. A. Yusof, J. Abdullah, U. Hashim and R. Hajian, *IEEE Sens. J.*, 2015, **15**(8), 4420–4427.
102 C.-C. Wu, H.-Y. Yen, L.-T. Lai, G.-C. Perng, C.-R. Lee and S.-J. Wu, *Sensors*, 2020, **20**(13), 3728.
103 S. Vinayagam, P. Rajaiah, A. Mukherjee and C. Natarajan, *Spectrochim. Acta, Part A*, 2018, **202**, 346–351.
104 F. M. Yrad, J. M. Castañares and E. C. Alocilja, *Diagnostics*, 2019, **9**(3), 74.
105 N. A. S. Omar, Y. W. Fen, S. Saleviter, Y. M. Kamil, W. M. E. M. M. Daniyal, J. Abdullah and M. A. Mahdi, *Sens. Actuators, A*, 2020, **303**, 111830.
106 Y. M. Kamil, S. H. Al-Rekabi, M. H. Yaacob, A. Syahir, H. Y. Chee, M. A. Mahdi and M. H. A. Bakar, *Sci. Rep.*, 2019, **9**(1), 13483.
107 Y. M. Kamil, M. H. A. Bakar, M. A. Mustapa, M. H. Yaacob, N. H. Z. Abidin, A. Syahir, H. J. Lee and M. A. Mahdi, *Sens. Actuators, B*, 2018, **257**, 820–828.
108 N. A. S. Omar, Y. W. Fen, J. Abdullah, M. H. M. Zaid, W. M. E. M. M. Daniyal and M. A. Mahdi, *Opt. Laser Technol.*, 2019, **114**, 204–208.
109 O. Adegoke and E. Y. Park, *J. Mater. Chem. B*, 2017, **5**(16), 3047–3058.

110 F. C. C. L. Loureiro, H. Neff, E. U. K. Melcher, R. A. Roque, R. M. P. de Figueiredo, C. Thirstrup, M. B. Borre and A. M. N. Lima, *Sens. Bio-Sens. Res.*, 2017, **13**, 96–103.
111 J. P. Chambers, B. P. Arulanandam, L. L. Matta, A. Weis and J. J. Valdes, *Curr. Issues Mol. Biol.*, 2008, **10**, 1–12.
112 L. S. Liu, F. Wang, Y. Ge and P. K. Lo, *ACS Appl. Mater. Interfaces*, 2021, **13**(8), 9329–9358.
113 K. L. Cox, V. Devanarayan and A. Kriauciunas, *et al.*, *The Assay Guidance Manual: Immunoassay Methods*, Eli Lilly & Company and the National Center for Advancing Translational Sciences, Bethesda (MD), 2012.
114 M. Majdinasab, M. Badea and J. L. Marty, *Pharmaceuticals*, 2022, **15**(1), 90.
115 B. Chakraborty, S. Das, A. Gupta, Y. Xiong, V. T-V, M. E. Kizer, J. Duan, A. R. Chandrasekaran and X. Wang, *ACS Infect. Dis.*, 2022, **8**, 667–692.
116 C. Tuerk and L. Gold, *Science*, 1990, **249**(4968), 505–510.
117 A. D. Ellington and J. W. Szostak, *Nature*, 1990, **346**, 818–822.
118 R. G. Ingle, S. Zeng, H. Jiang and W.-J. Fang, *J. Pharm. Anal.*, 2022, **12**, 517–529.
119 S. D. Jayasena, *Clin. Chem.*, 1999, **45**(9), 1628–1650.
120 D. J. Chinchilla-Cárdenas, J. S. Cruz-Méndez, J. M. Petano-Duque, R. O. García, L. R. Castro, M. J. Lobo-Castañón and G. O. Cancino-Escalante, *J. Genet. Eng. Biotechnol.*, 2024, **22**, 100400.
121 H. Yu, J. Zhu, G. Shen, Y. Deng, X. Geng and L. Wang, *Mikrochim. Acta*, 2023, **190**, 255.
122 M. Kohlberger and G. Gadermaier, *Biotechnol. Appl. Biochem.*, 2022, **69**, 1771–1792.
123 B. B. Junior, M. R. Batistuti, A. S. Pereira, E. M. de Sousa Russo and M. Mulato, *Talanta*, 2021, **233**, 122527.
124 K. H. Lee and H. Zeng, *Anal. Chem.*, 2017, **89**, 12743–12748.
125 B. B. Junior, M. R. B. Sawazaki and M. Mulato, *Mikrochim. Acta*, 2024, **191**, 72.
126 R. Thevendran, S. Rogini, G. Leighton, A. Mutombwera, S. Shigdar, T.-H. Tang and M. Citartan, *Biology*, 2023, **12**(5), 722.
127 C. R. Basso, B. P. Crulhas, M. Magro, F. Vianello and V. A. Pedrosa, *Talanta*, 2019, **197**, 482–490.
128 A. Chen and S. Yang, *Biosens. Bioelectron.*, 2015, **71**, 230–242.
129 P. S. Kwon, S. Ren, S.-J. Kwon, M. E. Kizer, L. Kuo, M. Xie, D. Zhu, F. Zhou, F. Zhang, D. Kim, K. Fraser, L. D. Kramer, N. C. Seeman, J. S. Dordick, R. J. Linhardt, J. Chao and X. Wang, *Nat. Chem.*, 2020, **12**, 26–35.
130 S. H. A. Gandham, D. E. Volk, G. L. R. Lokesh, M. Neerathilingam and D. G. Gorenstein, *Biochem. Biophys. Res. Commun.*, 2014, **453**, 309–315.
131 K. Matsunaga, M. Kimoto, V. W. Lim, H. P. Tan, Y. Q. Wong, W. Sun, S. Vasoo, Y. S. Leo and I. Hirao, *Nucleic Acids Res.*, 2021, **49**, 11407–11424.
132 K. Matsunaga, M. Kimoto, V. W. Lim, T.-L. Thein, S. Vasoo, Y.-S. Leo, W. Sun and I. Hirao, *Sci. Rep.*, 2021, **11**, 18000.
133 H. H. Nguyen, S. H. Lee, U. J. Lee, C. D. Fermin and M. Kim, *Materials*, 2019, **12**, 121.
134 M. Moharana, S. K. Pattanayak, F. Khan and S. Dave, in *Point-of-Care Biosensors for Infectious Diseases*, ed. S. Dave and J. Das, WILEY-VCH, India, 2023, ch. 1, pp. 1–14. DOI: 10.1002/9783527837946.ch1.
135 S. J. Fletcher, L. W. Phillips, A. S. Milligan and S. J. Rodda, *Biosens. Bioelectron.*, 2010, **26**, 1696–1700.
136 J. B. Biggins, J. R. Prudent, D. J. Marshall and J. S. Thorson, in *Fluorescent Energy Transfer Nucleic Acid Probes: Designs and Protocols*, ed. V. V. Didenko, Humana Press, Totowa, NJ, 2006, pp. 83–92. DOI: 10.1385/1-59745-069-3:83.
137 S. K. Chan, Y. S. Choong, D. Perera and T. S. Lim, *Anal. Methods*, 2018, **10**(2), 214–222.
138 F. Ghasemi, N. Fahimi-Kashani, A. Bigdeli, A. H. Alshatteri, S. Abbasi-Moayed, S. H. Al-Jaf, M. Y. Merry, K. M. Omer and M. R. Hormozi-Nezhad, *Anal. Chim. Acta*, 2023, **1238**, 340640.
139 H. Shand, S. Dutta, S. Rajakumar, S. J. Paulraj, A. K. Mandal, R. D. K. T. and K. T. R. Devi, *Front. Nanotechnol.*, 2022, **3**, 814550.
140 P. Damborský, J. Švitel and J. Katrlík, *Essays Biochem.*, 2016, **60**, 91–100.
141 A. Uniyal, G. Srivastava, A. Pal, S. Taya and A. Muduli, *Plasmonics*, 2023, **18**, 735–750.
142 M. Puiu and C. Bala, *Sensors*, 2016, **16**, 870.
143 H. H. Nguyen, J. Park, S. Kang and M. Kim, *Sensors*, 2015, **15**, 10481–10510.
144 X. Huang and M. A. El-Sayed, *J. Adv. Res.*, 2010, **1**, 13–28.
145 Y.-C. Yeh, B. Creran and V. M. Rotello, *Nanoscale*, 2012, **4**(6), 1871–1880.
146 K. A. Willets and R. P. Van Duyne, *Annu. Rev. Phys. Chem.*, 2007, **58**, 267–297.
147 J. Jatschka, A. Dathe, A. Csáki, W. Fritzsche and O. Stranik, *Sens. Bio-Sens. Res.*, 2016, **7**, 62–70.
148 E. Hutter and J. H. Fendler, *Adv. Mater.*, 2004, **16**, 1685–1706.
149 E. Petryayeva and U. J. Krull, *Anal. Chim. Acta*, 2011, **706**, 8–24.
150 S. Unser, I. Bruzas, J. He and L. Sagle, *Sensors*, 2015, **15**, 15684–15716.
151 J.-F. Masson, *ACS Sens.*, 2017, **2**(1), 16–30.
152 A. M. Shrivastav, U. Cvelbar and I. Abdulhalim, *Commun. Biol.*, 2021, **4**, 70.
153 P. P. Austin Suthanthiraraj and A. K. Sen, *Biosens. Bioelectron.*, 2019, **132**, 38–46.
154 I. Alejo-Cancho, J. Navero-Castillejos, A. Peiró-Mestres, R. Albarracín, J. Barrachina, A. Navarro, V. Gonzalo, V. Pastor, J. Muñoz and M. J. Martínez, *PLoS Neglected Trop. Dis.*, 2020, **14**, e0008082.
155 Z. L. Chong, S. D. Sekaran, H. J. Soe, D. Peramalah, S. Rampal and C.-W. Ng, *BMC Infect. Dis.*, 2020, **20**, 210.
156 D. Zhu, B. Liu and G. Wei, *Biosensors*, 2021, **11**, 259.
157 J. L. Montaño-Priede, M. Sanromán-Iglesias, N. Zabala, M. Grzelczak and J. Aizpurua, *ACS Sens.*, 2023, **8**(4), 1827–1834.

158 E. M. Linares, L. T. Kubota, J. Michaelis and S. Thalhammer, *J. Immunol. Methods*, 2012, **375**, 264–270.
159 K. Jiang, J.-H. Lee, T. S. Fung, J. Wu, C. Liu, H. Mi, R. P. V. J. Rajapakse, U. B. R. Balasuriya, Y.-K. Peng and Y. Y. Go, *Anal. Chim. Acta*, 2023, **1274**, 341565.
160 S. Alharthi, S. Alharthi, M. Madani, H. Alkhaldi, N. Aldaleeli, A. Almarri, F. Alnass, D. Alzahrani, S. A. Mahmoud, M. A. Haque, M. S. Attia, A. Siddiq, S. S. Aly and M. M. Ghobashy, *ChemBioEng Rev.*, 2025, **12**, e70006.
161 K. Girigoswami and N. Akhtar, *Int. J. Nano Dimens.*, 2019, **10**, 1–17.
162 C. E. Rowland, J. B. Delehanty, C. L. Dwyer and I. L. Medintz, *Mater. Today*, 2017, **20**, 131–141.
163 A. Boruah and B. K. Saikia, *J. Fluoresc.*, 2022, **32**, 863–885.
164 Z. R. Jones, N. J. Niemuth, Y. Zhang, C. R. Protter, P. C. Kinsley, R. D. Klaper and R. J. Hamers, *ACS Meas. Sci. Au*, 2022, **2**, 351–360.
165 C. D. Geddes and J. R. Lakowicz, *J. Fluoresc.*, 2002, **12**, 121–129.
166 D. Semeniak, D. F. Cruz, A. Chilkoti and M. H. Mikkelsen, *Adv. Mater.*, 2023, **35**, 2107986.
167 G. Park, H. Park, S.-C. Park, M. Jang, J. Yoon, J.-H. Ahn and T. Lee, *Nanomaterials*, 2023, **13**(2), 361.
168 S. Korposh, S. W. James, S.-W. Lee and R. P. Tatam, *Sensors*, 2019, **19**(10), 2294.
169 G. L. Machado, F. M. F. Teixeira, G. S. C. Ferreira, A. F. Versiani, L. M. Andrade, L. O. Ladeira, F. G. da Fonseca and J. C. Ramirez, *Part. Part. Syst. Charact.*, 2022, **39**, 2100157.
170 P. K. Jain, K. S. Lee, I. H. El-Sayed and M. A. El-Sayed, *J. Phys. Chem. B*, 2006, **110**, 7238–7248.
171 S. Link and M. A. El-Sayed, *Annu. Rev. Phys. Chem.*, 2003, **54**, 331–366.
172 J. A. Copland, M. Eghtedari, V. L. Popov, N. Kotov, N. Mamedova, M. Motamedi and A. A. Oraevsky, *Mol. Imaging Biol.*, 2004, **6**, 341–349.
173 D. Pissuwan, S. M. Valenzuela and M. B. Cortie, *Biotechnol. Genet. Eng. Rev.*, 2008, **25**, 93–112.
174 H. de Puig, J. O. Tam, C.-W. Yen, L. Gehrke and K. Hamad-Schifferli, *J. Phys. Chem. C*, 2015, **119**(30), 17408–17415.
175 A. L. Siegel and G. A. Baker, *Nanoscale Adv.*, 2021, **3**, 3980–4004.
176 W. Zhang, H. Duan, R. Chen, T. Ma, L. Zeng, Y. Leng and Y. Xiong, *Talanta*, 2019, **194**, 604–610.
177 C. Rodriguez-Quijada, J. Gomez-Marquez and K. Hamad-Schifferli, *ACS Nano*, 2020, **14**, 6626–6635.
178 A. Kudelski, *Talanta*, 2008, **76**, 1–8.
179 K. C. Bantz, A. F. Meyer, N. J. Wittenberg, H. Im, Ö. Kurtuluş, S. H. Lee, N. C. Lindquist, S.-H. Oh and C. L. Haynes, *Phys. Chem. Chem. Phys.*, 2011, **13**(24), 11551–11567.
180 L. Privitera, I. Paraboschi, K. Cross and S. Giuliani, *Front. Pediatr.*, 2021, **9**, 777840.
181 R. A. Tripp, R. A. Dluhy and Y. Zhao, *Nano Today*, 2008, **3**, 31–37.
182 K. Kant and S. Abalde-Cela, *Biosensors*, 2018, **8**, 62.
183 X. X. Han, R. S. Rodriguez, C. L. Haynes, Y. Ozaki and B. Zhao, *Nat. Rev. Methods Primers*, 2022, **1**, 87.
184 A. Y. F. Mahmoud, C. J. Rusin and M. T. McDermott, *Analyst*, 2020, **145**, 1396–1407.
185 M. Sánchez-Purrà, M. Carré-Camps, H. de Puig, I. Bosch, L. Gehrke and K. Hamad-Schifferli, *ACS Infect. Dis.*, 2017, **3**, 767–776.
186 A. F. Versiani, E. M. N. Martins, L. M. Andrade, L. Cox, G. C. Pereira, E. F. Barbosa-Stancioli, M. L. Nogueira, L. O. Ladeira and F. G. da Fonseca, *Sci. Rep.*, 2020, **10**(11302).
187 A. Schütz, F. Bernhard, N. Berrow, J. F. Buyel, F. Ferreira-da-Silva, J. Haustraete, J. van den Heuvel, J.-E. Hoffmann, A. de Marco, Y. Peleg, S. Suppmann, T. Unger, M. Vanhoucke, S. Witt and K. Remans, *STAR Protoc.*, 2023, **4**, 102572.
188 T. Trakoolwilaiwan, Y. Takeuchi, T. S. Leung, M. Sebek, L. Storozhuk, L. Nguyen, L. D. Tung and N. T. K. Thanh, *Nanoscale*, 2023, **15**, 12915–12925.
189 J. X. Wang, X. W. Sun, A. Wei, Y. Lei, X. P. Cai, C. M. Li and Z. L. Dong, *Appl. Phys. Lett.*, 2006, **88**(23), 233106.
190 M. Willander, O. Nur, Q. X. Zhao, L. L. Yang, M. Lorenz, B. Q. Cao, J. Z. Pérez, C. Czekalla, G. Zimmermann, M. Grundmann, A. Bakin, A. Behrends, M. Al-Suleiman, A. El-Shaer, A. C. Mofor, B. Postels, A. Waag, N. Boukos, A. Travlos, H. S. Kwack, J. Guinard and D. L. S. Dang, *Nanotechnology*, 2009, **20**, 332001.
191 P. Pormrungruang, S. Phanthanawiboon, S. Jessadaluk, P. Larpthavee, J. Thaosing, A. Rangkasikorn, N. Kayunkid, U. Waiwijit, M. Horprathum, A. Klamchuen, T. Pruksamas, C. Puttikhunt, T. Yasui, M. Djamal, S. Rahong and J. Nukeaw, *Nanomaterials*, 2023, **13**(21), 2846.
192 S. Tiwari, M. Vinchurkar, V. R. Rao and G. Garnier, *Sci. Rep.*, 2017, **7**, 43905.
193 X. Yu, Y. Xia, Y. Tang, W.-L. Zhang, Y.-T. Yeh, H. Lu and S.-Y. Zheng, *Small*, 2017, **13**(24), 1700425.
194 Y. Xia, Y. Chen, Y. Tang, G. Cheng, X. Yu, H. He, G. Cao, H. Lu, Z. Liu and S.-Y. Zheng, *ACS Sens.*, 2019, **4**, 3298–3307.
195 J. D. Bishop, H. V. Hsieh, D. J. Gasperino and B. H. Weigl, *Lab Chip*, 2019, **19**, 2486–2499.
196 H.-L. Chen, W.-H. Hsiao, H.-C. Lee, S.-C. Wu and J.-W. Cheng, *PLoS One*, 2015, **10**(6), e0131240.
197 T. Zhu, J. He, W. Chen, H. P. Ho, S. K. Kong, C. Wang, J. Long, J. Loo and D. Gu, *Anal. Biochem.*, 2018, **556**, 112–118.

